Science of the Total Environment 839 (2022) 156286

Contents lists available at ScienceDirect

Science of the Total Environment

journal homepage: www.elsevier.com/locate/scitotenv

Anthropogenic metal loads in nearshore sediment along the coast of China mainland interacting with provincial socioeconomics in the period 1980–2020

Xun Liu [a,b], Shen Yu [a,*]

[a] Institute of Urban Environment, Chinese Academy of Sciences, Xiamen 361021, China
[b] University of Chinese Academy of Sciences, Beijing 100049, China

HIGHLIGHTS

- Metal loads in sediment of China coast in literature were summarized in 1980–2020.
- Provincial pattern was evident for anthropogenic metal loads in nearshore sediment.
- Only Guangdong had medium-to-high risks of metal loads in sediment to Class I.
- Metal loads in nearshore sediment were highly related to metal emission industries.
- Few provinces achieved the EKC fittings between metal risks and NAGDP per capita.

GRAPHICAL ABSTRACT

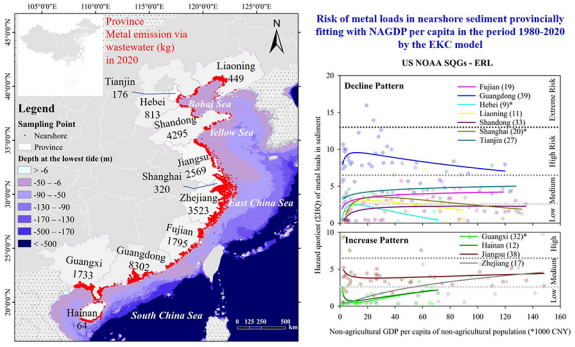

ARTICLE INFO

Editor: Xinbin Feng

Keywords:
Metals
Nearshore sediment
Socioeconomics
Interactions
Environmental Kuznets Curve (EKC) model
Risk assessment

ABSTRACT

Metal pollutions have been accused of consequences of the anthropogenic activities but few quantitative delineations between environmental metal loads and socioeconomic development presented. A meta-data analysis study was carried out on metal loads in coastal sediment in the provinces of China mainland reported in literature in the period 1980–2020. Eight metals with well-recognized anthropogenic sources were selected including arsenic (As), cadmium (Cd), chromium (Cr), copper (Cu), mercury (Hg), nickel (Ni), lead (Pb), and zinc (Zn). Screened with three criteria, a total of 1173 records from 405 published studies were finalized as the metal loads dataset in coastal sediment. Evident provincial patterns were observed among the selected metals but element dependent after transformed to sample number weighted contents (C_w). Against the regional marine backgrounds, anthropogenic increment rate ($R_{anthrop}$) of metal loads in nearshore sediment presented better provincial differentiation with the extremes at 7.58 for As and 62.13 for Cu in Guangdong, 91.25 for Hg in Zhejiang, 3.19 for Ni in Tianjin, 7.72 for Pb in Fujian, and 13.51 for Zn in Liaoning. Metal loads in coastal sediment could be explained by characteristic industries in the provinces. Nearshore sediment in Guangdong had high risk to metal loads and other provinces at low-to-medium risk to the lowest thresholds of sediment quality guidelines in China and USA. Canonical correlations identified considerably interactive explanations between integrative hazard quotients (ΣHQ) of the selected metals in nearshore sediment and non-agricultural GDP per capita of non-agricultural population/urban population percentile provincially but few significant fittings by the classic environmental Kuznets Curve model quantitatively. Findings of this study explored uncertainty from both sides in explaining the interactions, i.e., data integrity of metal loads in coastal sediment in literature and appropriation of socioeconomic indicators in relation to metal emission industries.

* Corresponding author.
E-mail address: syu@iue.ac.cn (S. Yu).

http://dx.doi.org/10.1016/j.scitotenv.2022.156286
Received 5 March 2022; Received in revised form 22 May 2022; Accepted 24 May 2022
Available online 26 May 2022
0048-9697/© 2022 Elsevier B.V. All rights reserved.

1. Introduction

Nearly 40% of the world population lives within 100 km from the coastline (Maul and Duedall, 2019), which hosts 22 out of 36 world megacities (over 10 million urban population) by 2021 with approximately 412 million urban populations according to the 17th Annual Edition of World Urban Areas by Demographia (www.demographia.com/db-worldua.pdf). Megacities and large urban agglomerations in the coast have led to considerable multi-challenges to the environments (von Glasow et al., 2013). Meanwhile, the inbound rivers also transport pollutants, especially nutrients and metals, from their upstream watersheds (Lin and Yu, 2018).

Heavy metals are of great global concern due to their bio-accumulable and toxic characteristics and non-biodegradability in the aquatic environment. Metals were found broadly enriched in tissue and shell of bivalve and gastropod shellfish from estuaries (Liu et al., 2022). Abnormal "colored oyster" (*Crassostrea hongkongensis*) is a typic bio-accumulative evidence indicating severe metal contaminations in estuaries, mainly copper (Cu), zinc (Zn), nickel (Ni), and chromium (Cr) (Weng and Wang, 2019). The United States Environmental Protection Agency (USEPA) has listed arsenic (As), cadmium (Cd), Cr, Cu, mercury (Hg), Ni, lead (Pb), and Zn as priority control pollutants (USEPA, 2014). Sedimentary metal records in coastal ecosystems were highly linked to anthropogenic impacts (Feng et al., 2011; Sun et al., 2019). The most highlighted anthropogenic activities in relation to sedimentary metals included land use changes (Yu et al., 2014), energy consumption (Li et al., 2012a), vehicular exhausts (Ma et al., 2016), waste recycling (Song and Li, 2014), and agricultural practices (Ouyang et al., 2018). Numerous studies found that sedimentary metal loads were significantly declined along the urban-rural gradient (Li et al., 2012b; Li et al., 2013; Simon et al., 2014; Ma et al., 2016). These findings hint that sedimentary metal loads in the coast might be highly associated with socioeconomic development in a region, such as an upstream watershed (Tang et al., 2005; Yu et al., 2014). However, interactions between metal loads in coastal sediment and socioeconomic development in a regional catchment or watershed have been scarcely argued.

Classically, the interactions of socioeconomic development and environmental change have been delineated by the Environmental Kuznets Curve (EKC) model, an inverse U-shaped curve (Stern, 2004). In the EKC model, the socioeconomic indicator is income (wealth) or gross domestic product (GDP) per capita instead of land uses or impervious surface area in the urban-rural gradient studies (Duan et al., 2015; Sharley et al., 2016; Taka et al., 2016). The EKC model had abundant fitting successes, for instance, atmospheric Cr emissions in Singapore over 120 years (Chen and Taylor, 2020), but a great number of failures were reported due to using the fixed socioeconomic indicator (Gergel et al., 2004; Capps et al., 2016; Chen and Xu, 2017; Kim et al., 2018). Zhou et al. (2019) identified non-agricultural GDP per capita of non-agricultural population (NAGDP per capita) with better EKC fitness to statistic discharges of chemical oxygen demand (COD) and ammonia per GDP unit at a watershed scale instead of GDP per capita classically. It was further confirmed by an EKC simulation between the measured ΣDDT and ΣPCB in estuarine sediment and NAGDP per capita in watershed (Hong et al., 2021).

China mainland has 11 coastal provinces and municipalities, approximately 13.5% of the national territory area, which hosted 44.8% of the national population and contributed 52.8% of the national GDP by 2019 before the COVID-19 pandemic, according to the National Bureau of Statistics of China (http://www.stats.gov.cn). The coast has been the frontline of China mainland with rapid economic development since 1978 following the reform and opening-up policy (Xie, 2020). In the past 40+ years, a huge volume of literature reported that the coastal environments in China mainland were contaminated with various pollutants, especially heavy metals in sediment (Cheung et al., 2003; Wang et al., 2013; Zhuang and Gao, 2014; Cao et al., 2015; Liang et al., 2016; Wang et al., 2016; Sun et al., 2019; Zhang et al., 2019b). Meanwhile, review articles were available for heavy metal pollution in sediment of China mainland coast, such as Bohai Sea (Gao et al., 2014), East China Sea (Fang and Lien, 2020), South China Sea (Wang et al., 2013), and the whole coast (Pan and Wang, 2012). These studies made a great number of historic metal records in coastal sediment available to explore socioeconomic pattern of coastal metal loads along the coast of China mainland via coupling the economic data in the 40+ year period, which were publicized by the National Bureau of Statistics (data.stats.gov.cn). An early study analyzed impacts of economic growth on coastal ecosystems of China mainland in the period 1950s–2010 and pointed out further degradation would be accelerated with development (He et al., 2014). This study aims to generate a long-term spatial dataset of metal loads in coastal sediment via compiling the published historic studies in China mainland in the period 1980–2020 for the priority control metals (As, Cd, Cr, Cu, Hg, Ni, Pb, and Zn). It is hypothesized that spatiotemporal patterns of these metal loads in sediment would be highly impacted by socioeconomic development in the coastal provinces, among which diverse and uneven structures of socioeconomic development coexisted in the past decades (Heilig, 2006). To comprehensively illustrate the environmental risk of metal loads in the coast, a special hazard quotient (ΣHQ) was calculated to integrate all the investigated metals against sediment quality guidelines (SQGs) of China and the USA. The interactions between metal load risks (ΣHQ) in coastal sediment and provincial economic development would be expressed by the EKC model fittings provincially. Given the rapid urbanization happened in the past decades, provincial urban population percentile was included as an indicator of socioeconomics with the economic indicators (GDP per capita, agricultural GDP per capita of agricultural population (AGDP per capita), and NAGDP per capita). Findings of this study would enhance understandings quantitatively on environmental impacts of socioeconomic development for policy- and decision-makers, who will strategize low-impact development policies in the future.

2. Materials and methods

2.1. Data collection

2.1.1. Metal load data

Historic records were collected from the national marine surveys in 1980s (National Coastal Zone Office of China, 1989), 1990s (Editorial Board of National Comprehensive Survey of Island Resources, 1996), and 2000s (Editorial Board of Comprehensive Investigation and Assessment in Offshores of China, 2012). Meanwhile, a systematic literature search was conducted using the Web of Science (WOS) and China National Knowledge Infrastructure (CNKI) databases covering 11 coastal provinces and municipalities of China mainland (i.e., Liaoning, Hebei, Tianjin, Shandong, Jiangsu, Shanghai, Zhejiang, Fujian, Guangdong, Guangxi, and Hainan) (Fig. 1). An entry of keywords stated as "'heavy metal OR arsenic OR cadmium OR chromium OR copper OR mercury OR nickel OR lead OR zinc' AND 'estuary OR coast OR sea OR bay OR port OR mangrove OR intertidal' and 'China'" with a period "Year = 1980–2020". The searched articles were filtered by the following criteria: 1) containing total contents of any metals (As, Cd, Cr, Cu, Hg, Ni, Pb, or Zn) in estuarine or coastal sediment (surficial sediment or sediment core) of China mainland in mean or median with standard deviation (SD) or standard error (SE); 2) containing geographic information of sampling sites/points with longitude, latitude, and depth, and sampling time including dating year of sediment cores; 3) containing information of reliable chemical analysis methods and analytical instruments for metal quantification with quality assurance and quality control (QA/QC). A workflow diagram could be found in Fig. S1 in the Supplementary Materials. In total, 405 published studies (or articles) met the criteria with 1173 mean records of metal loads from 56,468 surface sediment samples and top layer of sediment cores. Part of the data without reporting values was extracted from figures of the selected articles using the GetData Graph Digitizer (Ver. 2.26, http://www.getdata-graph-digitizer.com). The majority of sediment samples were collected in shallow sea within a depth <90 m, classified into nearshore (water depth ≤ 6 m at the lowest tide) and offshore (water depth > 6 m) categories (Fig. 1). Overall, total content of metals was quantified in mixed acid digests (mixing

two, three and even four concentrated acids as nitric acid, hydrogen fluoride, perchloric acid, and chloric acid and few adding hydrogen peroxide) using inductively coupled plasma (ICP) with mass (MS) or atomic/optical emission spectrometry (A/OES), atomic absorption spectroscopy (AAS), or atomic fluorescence spectroscopy (AFS). Part of data was determined using X-ray fluorescence (XRF) with boric acid tablet.

2.1.2. Socioeconomic data

Yearly records of GDP and components, population and urban population were collected for all the coastal provinces in the period 1980–2020 at https://data.stats.gov.cn. Socioeconomic indicators were calculated as GDP per capita, agricultural GDP per capita of agricultural population (AGDP per capita), non-agricultural GDP per capita of non-agricultural population (NAGDP per capita), and urban population percentile. NAGDP is the difference between GDP and agricultural GDP.

2.2. Calculation of indicators

2.2.1. Weighted metal content (C_w)

The collected data were mean values of various number samples over time. To express metal loads provincially (or nationally) and yearly in the period 1980–2020, a sample-number weighted content of each selected metal (C_w) was calculated to illustrate the overall metal-load status in coastal sediment as the following equation (Eq. (1), Niu et al., 2020):

$$C_w = \frac{\sum_{i=1}^{n} C_i \times N_i}{\sum_{i=1}^{n} N_i} \quad (1)$$

where C_i is the collected mean record i, N_i is number of samples in the collected mean record i, n is number of the collected mean records.

2.2.2. Anthropogenic increment rate ($R_{anthrop}$)

Anthropogenic increment rate was calculated against the geological or environmental background of each selected metal provincially as the following equation (Eq. (2), Han et al., 2019):

$$R_{anthrop} = \frac{C_w - C_{backgroud}}{C_{background}} \quad (2)$$

where C_w is the sample number weighted mean of each selected metal of province or nation (Eq. (1)), and $C_{background}$ is the background value of each selected metal in the shallow marine sediment of each province within the four marine zones (Ji, 2011). The provincial background values of the selected metals (Ni not available) were taken from the reported background values of the adjunct seas, i.e., Bohai Sea for Liaoning, Hebei, and Tianjin, Yellow Sea for Shandong and Jiangsu, East China Sea for Shanghai,

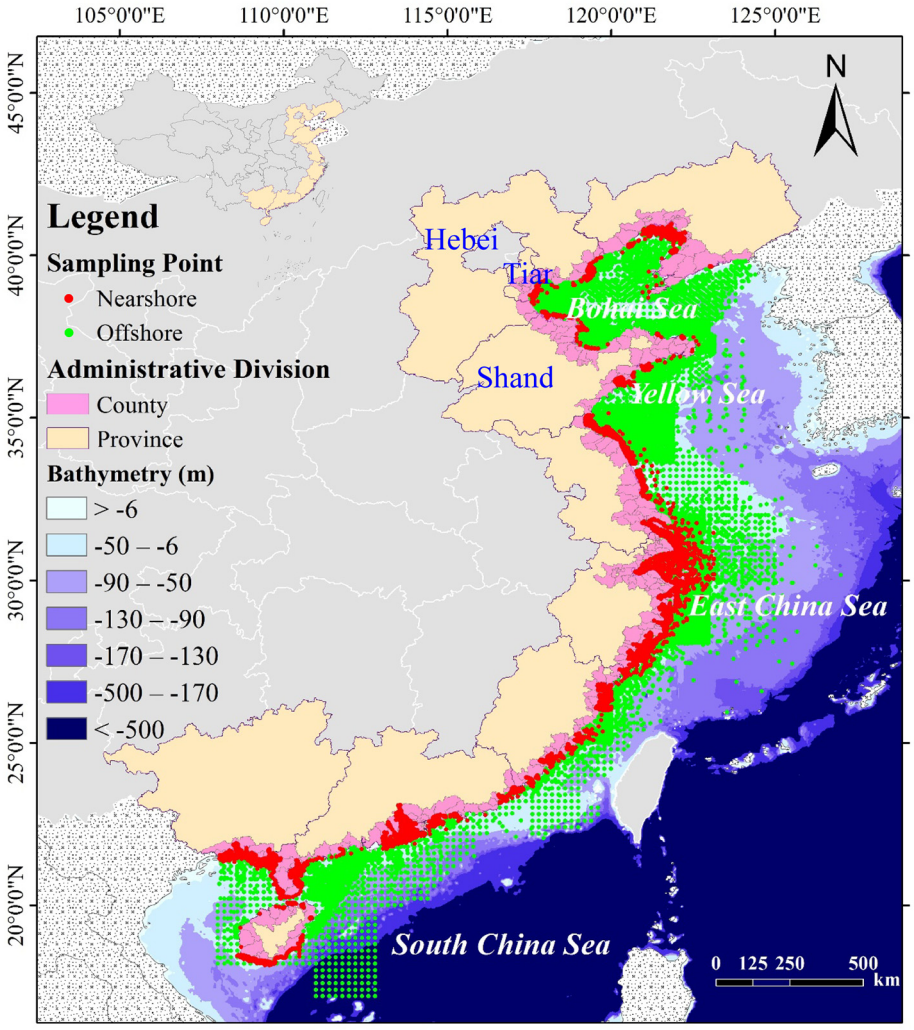

Fig. 1. Distribution of coastal sediment sampling points along the coast of China mainland in the period 1980–2020 reported in the literature. The sampling points were divided into nearshore (<6 m depth at the lowest tide) and offshore (>6 m depth at the lowest tide). The bathymetry was extracted from the ETOPO1 database by the Marine Geology and Geophysics of the National Oceanic and Atmospheric Administration (NOAA) of the United States (Amante and Eakins, 2009).

Zhejiang, and Fujian, and South China Sea for Guangdong, Guangxi, and Hainan (Ji, 2011). The background value of Ni for the calculation was obtained from the national one (24.0 mg kg^{-1}) for all the provinces (Zhao and Yan, 1993).

2.2.3. Specific hazard quotient (ΣHQ)

Comprehensive metal risk in sediment of the coast was assessed by a specific hazard quotient (Σ*HQ*), which was calculated as the following equation (Eq. (3), Piva et al., 2011):

$$HQ = \frac{\sum_{i=1}^{n}\left(\frac{C_{wi}}{(\text{Class I or ERL})_i} \times RW_i\right)_{\le 1}}{n} + \sum_{j=1}^{m}\left(\frac{C_{wj}}{(\text{Class I or ERL})_j} \times RW_j\right)_{>1} \quad (3)$$

where C_w is the sample number weighted mean of each selected metal of province or nation (Eq. (1)), n and m are numbers of the selected metals with a ratio of $(\frac{C_w}{\text{Class I or ERL}} \times RW) \le 1$ and >1, respectively; values of Class I and ERL (effect range low) are from the sediment quality guidelines of China (China-SQGs, GB18668-2002, General Administration of Quality Supervision, 2002) and of the United States (NOAA-SQGs, National Oceanic and Atmospheric Administration of the United States, 1999), respectively; *RW* is risk weight for each selected metal, i.e., 1.0 for As, Cr, Cu, and Zn; 1.1 for Ni and Pb; and 1.3 for Cd and Hg (Piva et al., 2011). The comprehensive metal risk in sediment was categorized into four classes by Σ*HQ*, i.e., low, moderate, major, and severe risk with Σ*HQ* ranging from 0 to <2.6, 2.6 to <6.5, 6.5 to <13, and ≥13, respectively (Piva et al., 2011).

2.2.4. Environmental Kuznets Curve model

A classic Environmental Kuznets Curve model was applied for delineating interactions between Σ*HQ* and the yearly provincial socioeconomic indicators (SI, i.e., non-agricultural GDP per capita of non-agricultural population (NAGDP per capita) and urban population percentile) following the model (Eq. (4), Stern, 2004):

$$\Sigma HQ = a + b \times \ln SI + c \times (\ln SI)^2 \quad (4)$$

2.3. Statistical analysis

Nonparametric one-way ANOVA with a Kruskal-Wallis test was employed to compare provincial differences for the sample number weighted content (C_w) (Eq. (1)) of the selected metal loads in coastal sediment and their anthropogenic increment rates ($R_{anthrop}$) (Eq. (2)). Interactions between $R_{anthrop}$ and provincial socioeconomics were tested using canonical redundancy analysis for each province and the national coast. The highly related socioeconomic indicators were identified for the EKC fitting with the special hazard quotients (Eq. (4)) of metal loads in coastal sediment provincially. The above statistical analyses were performed using SAS® OnDemand for Academics (SAS Institute Inc., Cary, NC, USA).

3. Results

3.1. Spatiotemporal changes of metal loads in coastal sediment of China mainland

Sedimentary loads of the selected 8 metals along the coast of China mainland showed diverse differences among the 11 coastal provinces (Table 1). Generally, the metals had more significant variations in the nearshore sediment (water depth less than 6 m at the lowest tide) than those in the offshore one except Hg with no statistical differences among the provinces for both nearshore and offshore ones. Yearly means and medians of each metal were summarized in Table 1 as well as the number of available years. Most nearshore records of metal loads in sediment were greater than the offshore ones but only few statistically significant ($p < 0.05$), and few significant reverse exceptions existed (Table 1). Among the 11 coastal provinces, Guangdong had significant greater loads of the selected metals (except Hg) in nearshore sediment over the period than others ($p < 0.05$, Table 1). The greatest records for the selected metal loads (C_w, sample number weighted content) in nearshore sediment were found in Tianjin (31.7 mg As kg^{-1} in 2009 and 76.6 mg Ni kg^{-1} in 2012), Guangdong (2.01 mg Cd kg^{-1} in 1991, 185 mg Cr kg^{-1} and 295 mg Cu kg^{-1} in 2014), Guangxi (0.81 mg Hg kg^{-1} in 1983), and Fujian (75.6 mg Pb kg^{-1} in 1990 and 327 mg Zn kg^{-1} in 1984).

Over the period 1980–2020, the trends of temporal changes in sedimentary metal content (C_w) depended upon metals and provinces. For instance, Guangdong with the greatest loads of all the selected metals had three temporal trends of sedimentary metal loads in nearshore, i.e., decline patterns for As, Cd, Cr, and Ni; increase patterns for Cu and Hg; and flat pattern for Zn (Fig. 2). Hebei was the province having decline temporal pattern for all the selected metals at various rates while Tianjin surrounded by Hebei had increase patterns for most of the selected metals over the period (Fig. 2).

The anthropogenic increment rates ($R_{anthrop}$) of the selected metal loads in coastal sediment against the regional background values provided better provincial differences than the content (C_w) (Table 2). Most provinces had $R_{anthrop}$ greater than 1.00, i.e., doubling the regional background values of metal loads in coastal sediment. The nearshore sediments had higher $R_{anthrop}$ than the offshore ones in most coastal provinces in agreement with C_w (Tables 1 and 2). Similarly, Guangdong had significantly greater $R_{anthrop}$ for As, Cd, Cu, and Ni loads in nearshore sediment than other provinces but $R_{anthrop}$ of Cr, Hg, Pb, and Zn were significantly higher in Shanghai, Zhejiang, Fujian, and Tianjin, respectively (Table 2). The extreme yearly $R_{anthrop}$ for the selected metal loads in nearshore sediment were found in Guangdong (7.58 for As in 1989 and 62.13 for Cu in 2014), Shanghai (43.25 for Cd in 2006 and 8.33 for Cr in 2000), Zhejiang (91.25 for Hg in 2019), Tianjin (3.19 for Ni in 2012), Fujian (7.72 for Pb in 1990), and Liaoning (13.51 for Zn in 2010).

3.2. Hazard risk assessment of metal loads in nearshore sediment in China mainland

According to the metal loads in sediment and the source–sink relationship, the metal loads in nearshore sediment were used for the hazard risk assessment. Except Guangdong, nearshore sediment in the provinces had only few yearly records of metal load (C_w) exceeding the threshold of China SQGs - Class I (Table 3). Sediment in Guangdong nearshore had Cd, Cr and Cu exceeders of the Class I at 28, 26, and 27 out of 39 yearly records as well as 15 out of 38 yearly records, but only 1 or 2 records exceeding the Class II and III (Table 3). In contrast to the US NOAA SQGs, more ERL exceeders of the yearly records in nearshore sediment of the provinces were identified due to the ERL thresholds of the selected metals less than the Class I except Cd (Table 3). The yearly records of Ni in nearshore sediment largely exceeded the ERL for all the provinces, such as Tianjin with 25 out of 25 yearly records, Guangdong with 39 out of 39 yearly records, Jiangsu with 36 out of 37 yearly records, Shanghai with 14 out of 19 yearly records, and Shandong with 11 out of 28 yearly records (Table 3).

On the other hand, hazard quotient (ΣHQ) of multiple metal loads (at least 4 metal records a year) in sediment also indicated that nearshore sediment in Guangdong had medium to high risk against China SQGs - Class I and high to extreme risk against US NOAA SQGs - ERL, and the rest provinces had metal loads in nearshore sediment with low–medium risk against both SQGs (Fig. 2). Guangdong had the greatest ΣHQ at 21.6 (China SQGs Class I) and 24.3 (US NOAA SQGs - ERL) in 2014 and ranked top for 6 and 10 years, followed by Shandong (7.49 and 10.0 in 2003) and Zhejiang (5.34 and 9.79 in 2019), respectively.

3.3. Interactions between metal loads in nearshore sediment and socioeconomic development in the coastal provinces of China mainland

The anthropogenic increment rate ($R_{anthrop}$) was used as an indicator of metal loads in nearshore sediment to explore interactions with

Table 1
Sample number weighted content (C_w, mg kg^{-1}) of the selected metal loads in coastal sediment yearly in China mainland in the period 1980–2020 reported in the literature.

Province[¶]	Item	As			Cd			Cr			Cu			Hg			Ni			Pb			Zn		
		Coast[§]	Near-shore	Off-shore	Coast	Near-shore	Off-shore	Coast	Near-shore	Off-shore	Coast	Near-shore	Off-shore	Coast	Near-shore	Off-shore	Coast	Near-shore	Off-shore	Coast	Near-shore	Off-shore	Coast	Near-shore	Off-shore
Liaoning	Year	11	8	6	14	11	8	11	9	7	14	12	8	12	9	6	5	2	4	14	12	8	14	12	8
	Mean	10.19	11.04	8.92	0.277	0.275	0.284	42.59	53.04	36.18	16.93	18.94	16.48	0.068	0.086	0.051	22.23	26.32	20.29	21.98	24.19	22.10	73.48	80.30	62.85
	Median	9.35	9.41	8.43	0.216	0.228	0.166	41.83	50.80	27.00	17.61	19.71	16.36	0.053	0.052	0.045	22.67	26.32	22.33	20.60	21.44	22.34	59.02	70.54	60.01
Hebei	Year	10	2	9	15	9	9	12	6	9	15	9	9	13	7	8	4	2	2	15	9	9	15	9	9
	Mean	9.05	9.55	9.06	0.256	0.324	0.154	37.00	34.97	34.39	18.18	16.73	17.92	0.058	0.071	0.041	27.03	25.59	28.48	17.07	17.89	17.39	45.27	44.03	44.00
	Median	8.31	9.55	8.31	0.148	0.130	0.158	33.66	34.56	33.61	16.43	15.50	16.33	0.040	0.031	0.043	25.59	25.59	28.48	16.54	16.10	17.60	42.71	42.25	42.71
Tianjin	Year	24	19	7	30	27	16	24	20	8	30	27	15	27	19	12	25	25	3	30	27	16	30	27	16
	Mean	11.95	12.34	9.49	0.216	0.219	0.227	64.61	64.83	67.81	30.29	31.68	30.56	0.061	0.070	0.065	38.68	38.86	36.00	25.62	27.57	24.23	89.11	93.16	94.49
	Median	11.52	11.50	9.87	0.162	0.170	0.179	65.65	65.85	62.42	31.72	31.96	31.40	0.039	0.022	0.049	37.38	38.93	34.40	25.62	26.90	22.39	88.35	91.32	93.03
Shandong	Year	19	18	13	33	33	13	19	19	13	33	33	13	30	27	12	31	28	8	33	33	13	33	33	13
	Mean	10.58	10.23	10.06	0.190	0.211	0.183	53.10	48.95	45.53	19.10	17.66	21.83	0.067	0.068	0.049	19.93	18.81	26.69	17.57	17.59	21.42	51.24	50.37	54.93
	Median	9.20	8.74	10.07	0.117	0.126	0.143	53.45	54.02	45.70	17.51	15.72	20.22	0.057	0.057	0.044	20.47	17.37	26.90	15.58	14.84	21.55	51.63	50.07	54.21
Jiangsu	Year	38	38	5	37	37	7	38	38	6	38	38	7	37	37	4	38	37	3	38	38	7	38	38	7
	Mean	12.45	12.62	16.17	0.261	0.258	0.360	60.36	62.22	57.60	19.92	20.72	17.43	0.052	0.055	0.020	35.34	35.85	32.14	23.55	24.14	23.52	63.25	63.79	92.09
	Median	11.97	12.34	11.30	0.184	0.184	0.206	61.27	63.34	61.85	18.43	18.70	19.84	0.041	0.044	0.019	33.68	35.20	31.89	22.92	23.47	20.27	58.93	60.03	66.80
Shanghai	Year	10	5	9	24	22	10	22	19	9	25	23	10	11	6	9	23	19	6	25	23	10	24	22	9
	Mean	9.69	11.18	9.36	0.157	0.181	0.141	73.68	77.73	63.96	24.19	24.22	23.46	0.054	0.067	0.047	27.35	25.32	35.62	20.29	19.23	24.08	74.64	75.72	77.29
	Median	9.69	10.10	9.40	0.161	0.164	0.137	75.63	78.90	70.65	20.42	18.26	23.20	0.054	0.068	0.050	22.55	21.84	33.73	21.17	14.75	23.91	67.88	65.72	77.19
Zhejiang	Year	16	14	9	20	18	12	15	13	10	20	18	13	19	16	10	11	7	7	29	18	22	19	17	13
	Mean	10.06	10.29	11.71	0.149	0.176	0.121	67.34	63.38	72.09	30.05	30.63	27.33	0.088	0.096	0.051	37.44	37.26	38.97	31.60	26.29	33.08	91.58	86.65	93.80
	Median	10.52	9.98	10.99	0.141	0.154	0.120	60.71	58.08	75.69	30.43	30.49	30.62	0.053	0.053	0.047	39.74	38.00	43.14	29.71	25.47	31.37	93.70	89.62	102.4
Fujian	Year	15	15	2	22	22	3	14	13	3	23	23	5	17	17	2	13	12	3	22	22	5	21	21	5
	Mean	9.34	9.43	9.10	0.210	0.232	0.069	55.40	48.71	80.26	27.93	29.73	22.11	0.069	0.068	0.076	34.04	32.17	39.23	42.53	44.07	33.48	130.6	135.9	127.2
	Median	9.34	9.57	9.10	0.160	0.184	0.068	49.98	47.66	68.90	25.32	26.84	20.28	0.067	0.067	0.076	33.01	30.61	37.10	42.22	43.54	35.52	112.1	112.1	98.76
Guangdong	Year	38	38	28	39	39	28	39	39	28	39	39	28	37	36	26	39	39	24	39	39	28	39	39	28
	Mean	15.51	17.68[η]	7.13	0.673	0.730	0.143	75.98	86.2	26.01	47.60	51.20	16.07	0.119	0.124	0.071	36.26	40.58	12.97	40.66	43.77	25.45	119.3	126.8	70.03
	Median	15.63	18.84	4.91	0.597	0.727	0.028	75.69	89.49	20.52	39.33	43.61	10.67	0.080	0.085	0.072	35.22	40.59	12.71	38.99	42.11	25.26	113.6	124.1	65.37
Guangxi	Year	32	32	5	32	32	5	9	9	3	32	32	4	32	32	5	2	2	nd[#]	32	32	5	30	30	3
	Mean	8.10	8.00	8.71	0.154	0.164	0.131	34.96	34.57	45.32	13.80	13.99	23.41	0.085	0.086	0.058	18.48	18.48	nd	22.01	22.01	26.61	46.39	46.05	56.84
	Median	7.68	7.34	7.82	0.127	0.128	0.120	33.41	33.41	44.42	13.86	13.89	13.35	0.063	0.063	0.060	18.48	18.48	nd	23.39	23.30	31.50	41.10	40.15	52.37
Hainan	Year	10	9	3	12	12	3	9	8	3	12	12	3	11	9	3	4	3	2	12	12	3	12	12	3
	Mean	8.06	8.42	8.58	0.356	0.370	0.220	42.88	46.95	31.58	16.89	19.78	10.27	0.059	0.048	0.085	17.93	24.28	12.70	26.25	26.65	19.68	67.17	70.05	50.34
	Median	8.67	9.29	9.50	0.168	0.261	0.119	40.23	46.52	33.90	15.61	18.69	9.12	0.040	0.040	0.030	15.63	29.79	12.70	26.81	26.81	22.74	69.80	69.80	59.40
Nation	Year	40	40	33	40	40	33	40	40	33	40	40	33	40	40	33	40	40	31	40	40	36	40	40	33
	Mean	12.01	12.83	7.29	0.299	0.328	0.136	66.30	69.31	36.86	27.95	29.04	19.08	0.090	0.095	0.060	32.42	34.31	20.65	30.36	31.84	26.34	90.89	92.33	78.70
	Median	12.15	12.72	5.78	0.252	0.261	0.124	64.74	70.22	24.15	25.24	26.85	19.32	0.059	0.061	0.055	32.82	34.99	15.29	27.50	28.40	26.23	84.31	87.60	72.81
Liaoning			BC*	AB		B	NS		BCD	CDE		BC	AB		NS	NS		ABC	CDE		BCD	ABC		BCDE	BCD
Hebei			AB	AB		B	NS		CD	DE		BC	AB		NS	NS		ACB	ABCD		BCD	C		DE	D
Tianjin			B	AB		B	NS		BC	AB		B	A		NS	NS		A	AB		B	BC		B	AB
Shandong			BC	AB		B	NS		C	BCDE		BC	AB		NS	NS		C	BCD		D	BC		DE	CD
Jiangsu			B	A		B	NS		BC	ABCD		BC	AB		NS	NS		A	ABC		BCD	ABC		CDE	ABC
Shanghai			ABC	AB		B	NS		AB	ABC		BC	AB		NS	NS		BC	AB		CD	ABC		BCD	ABC D
Zhejiang			BC	AB		B	NS		BC	A		BC	AB		NS	NS		AB	A		BC	A		BC	AB
Fujian			BC	AB		B	NS		CD	AB		BC	AB		NS	NS		AB	AB		A	AB		A	A
Guangdong			A	B		A	NS		A	E		A	B		NS	NS		A	E		A	ABC		A	BCD
Guangxi			C	AB		B	NS		D	ABCDE		C	AB		NS	NS		BC	nd[η]		BCD	ABC		E	BCD
Hainan			BC	AB		B	NS		CD	BCDE		BC	AB		NS	NS		ABC	DE		BCD	ABC		BCDE	BCD

[¶]Provinces were listed from north to south along the coast of China mainland.
[§]The samples were grouped into nearshore (depth ≤ 6 m at the lowest tide) and offshore (depth > 6 m at the lowest tide), and coast as a whole.
[η]Data in red indicated a significant difference of metal load in sediment where the loads in nearshore were larger than those in offshore and opposite for data in blue at $p < 0.05$ by nonparametric one-way ANOVA with a Kruskal-Wallis test ($Pr > Chi^2$).
[#]"nd" indicated "no data".
*Different letters indicate differences among the 11 provinces at a significance level at $p < 0.05$, explored by One-Way ANOVA with a Tukey's multi-comparison method, and NS represents "not significant" with yearly data as the replicates.

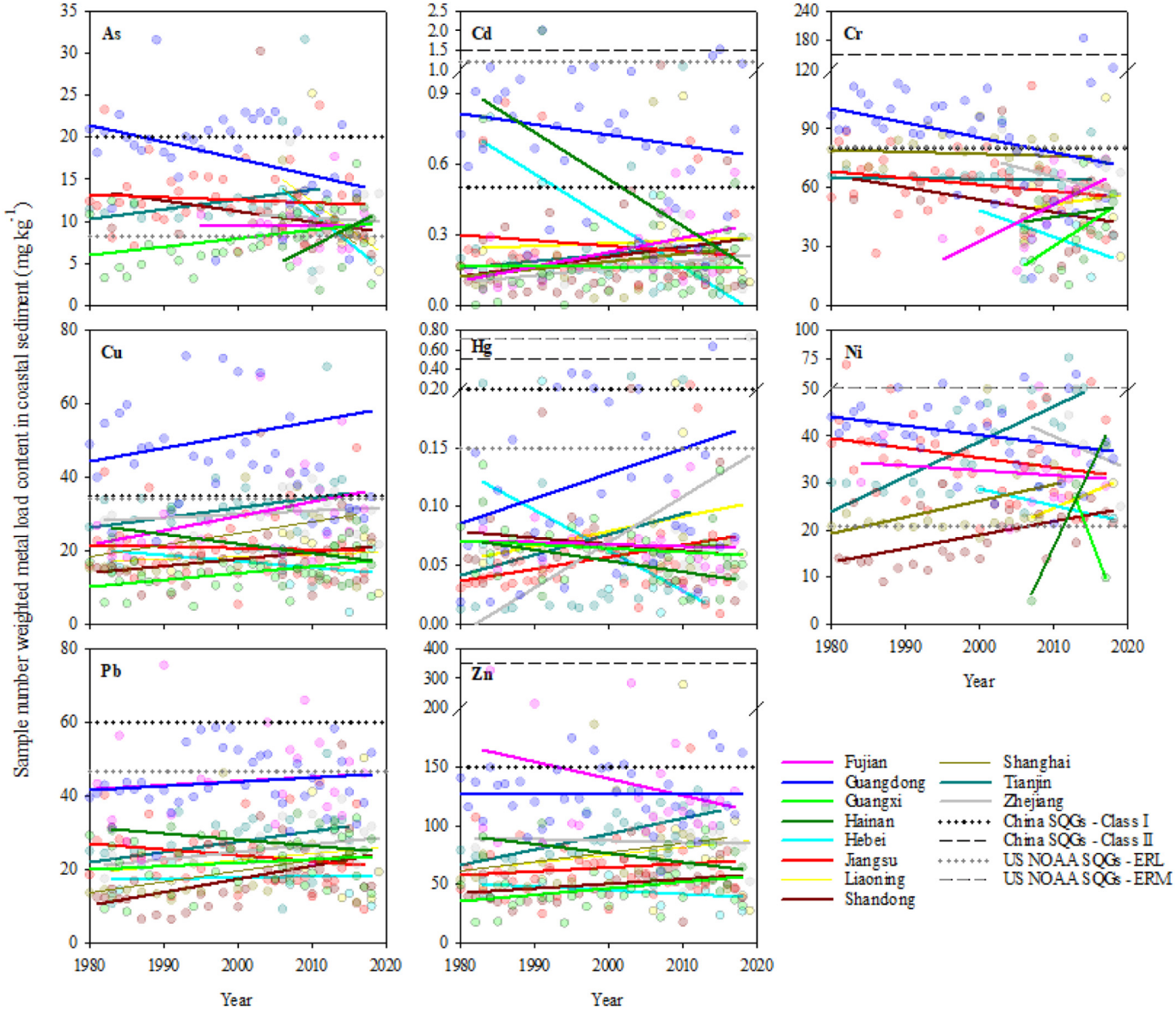

Fig. 2. Temporal changes of sample number weighted content (C_w) of the selected metals in nearshore sediment of China mainland in the period 1980–2020. The linear regression lines in color for each province only indicate change trends over the period. Thresholds of sediment quality guidelines (SQGs) for individual metals were presented according to China SQGs (GB18668-2002) and US NOAA SQGs.

socioeconomic development in the coastal provinces of China mainland due to the better provincial differentiation in comparison to C_w (Tables 1 and 2). According to the canonical redundancy analysis, interactive explanations between metal $R_{anthrop}$ and socioeconomics were remarkable on a north-to-south order in Hebei (29% versus 58%), Tianjin (32% versus 12%), Shandong (13% versus 26%), Shanghai (26% versus 58%), Zhejiang (21% versus 13%), Fujian (19% versus 17%), and Guangxi (13% versus 50%) (Table 4). Among the four socioeconomic indicators, urban population percentile and NAGDP per capita ranked on top in correlations to the canonical variables of metal $R_{anthrop}$. However, metals varied for the provinces in correlations to the canonical variables of socioeconomics, for instance, Cd in Hebei with the highest correlation efficient, Ni and Zn in Tianjin, Pb in Shandong, Ni in Shanghai, As, Cr, and Cu in Zhejiang, Cr, Cu, and Zn in Fujian, and As, Cu, and Zn in Guangxi, respectively (Table 4). Integrating the 11 coastal provinces, only Zn and urban population percentile had slight high correlation efficient to the opposite dataset, regardless of number of metals involved (Table 4).

To quantitatively delineate relationships between metal loads in nearshore sediment and industrialization/urbanization in the coastal provinces, the classic environmental Kuznets Curve (EKC) model was employed to fit the integrative indicator ΣHQ (a calculated overall risk value of multiple metal loads in sediment) and socioeconomic indicator (NAGDP per capita as economic development indicator or urban population percentile as urbanization one). NAGDP per capita and urban population percentile had been identified in high correlations to yearly anthropogenic increment rates of multiple metal loads in nearshore sediment ($R_{anthrop}$) for most provinces by canonical redundancy analysis (Table 4). Two sediment quality guidelines (SGQs) were used to calculate ΣHQ for status recognition (China SQGs) and international comparison (US NOAA SQGs). With fitting the EKC model, both ΣHQ calculated by China SQGs - Class I and US SQGs - ERL similarly had two patterns to NAGDP per capita, i.e., decline (inverse U shape) and increase (U shape) patterns (Fig. 3). But, the two SQGs categorized the 11 coastal provinces into different patterns. Guangdong, Hebei, Liaoning, Shandong, and Shanghai consistently showed the decline pattern while Guangxi, Jiangsu, and Zhejiang followed the increase pattern. Fujian, Hainan, and Tianjin were shifted between the two SQGs, possibly because that Ni was included in US SQGs. With the statistical test, only Shanghai had a significant EKC fitting ($p < 0.05$) between NAGDP per capita and

Table 2
Anthropogenic increment rate ($R_{anthrop}$) of the selected metal loads in coastal sediment yearly in China mainland in the period 1980–2020 reported in the literature.

Marine Zone	Province[¶]	Item	As			Cd			Cr			Cu			Hg			Ni			Pb			Zn		
			Coast	Near-shore	Off-shore	Coast	Near-shore	Off-shore	Coast	Near-shore	Off-shore	Coast	Near-shore	Off-shore	Coast	Near-shore	Off-shore	Coast	Near-shore	Off-shore	Coast	Near-shore	Off-shore	Coast	Near-shore	Off-shore
	Background (mg kg^{-1})[§]		7.06			0.120			23.10			16.50			0.025			24.00			14.60			20.70		
Bohai Sea	Liaoning	Year	11	8	6	14	11	8	11	9	7	14	12	8	12	9	6	5	2	4	14	12	8	14	12	8
		Mean	1.44	1.56	1.26	2.31	2.29	2.36	1.84	2.30	1.57	1.03	1.15	1.00	2.72	3.46	2.03	0.93	1.10	0.85	1.51	1.66	1.51	3.55	3.88	3.04
		Median	1.32	1.33	1.19	1.80	1.90	1.38	1.81	2.20	1.17	1.07	1.19	0.99	2.13	2.06	1.80	0.94	1.10	0.93	1.41	1.47	1.53	2.85	3.41	2.90
	Hebei	Year	10	2	9	15	9	9	12	6	9	15	9	9	13	7	8	4	2	2	15	9	9	15	9	9
		Mean	1.28	1.35	1.28	2.13	2.70	1.28	1.60	1.51	1.49	1.10	1.01	1.09	2.34	2.83	1.63	1.13	1.07	1.19	1.17	1.23	1.19	2.19	2.13	2.13
		Median	1.18	1.35	1.18	1.23	1.08	1.32	1.46	1.50	1.45	1.00	0.94	0.99	1.60	1.24	1.74	1.07	1.07	1.19	1.13	1.10	1.21	2.06	2.04	2.06
	Tianjin	Year	24	19	7	30	27	16	24	20	8	30	27	15	27	19	12	25	25	3	30	27	16	30	27	16
		Mean	1.69	1.75	1.34	1.80	1.83	1.89	2.80	2.81	2.94	1.84	1.92	1.85	2.43	2.81	2.61	1.61	1.62	1.50	1.76	1.89	1.66	4.30	4.50	4.56
		Median	1.63	1.61	1.40	1.35	1.38	1.49	2.84	2.85	2.70	1.92	1.94	1.90	1.56	0.90	1.96	1.56	1.63	1.43	1.75	1.85	1.53	4.27	4.58	4.49
	Background (mg kg^{-1})		6.82			0.203			27.20			7.03			0.013			24.00			21.30			32.60		
Yellow Sea	Shandong	Year	19	18	13	33	33	13	19	19	13	33	33	13	30	27	12	31	28	8	33	33	13	33	33	13
		Mean	1.55	1.50	1.47	0.93[η]	1.04	0.90	1.95	1.80	1.67	2.72	2.51	3.11	5.15	5.24	3.78	0.83	0.78	1.11	0.82	0.83	1.01	1.57	1.55	1.68
		Median	1.35	1.28	1.48	0.58	0.62	0.71	1.96	1.99	1.68	2.49	2.24	2.88	4.38	4.38	3.40	0.85	0.72	1.12	0.73	0.70	1.01	1.58	1.54	1.66
	Jiangsu	Year	38	38	5	37	37	7	38	38	6	38	38	7	37	37	4	38	37	3	38	38	7	38	38	7
		Mean	1.83	1.85	2.37	1.29	1.27	1.77	2.22	2.29	2.12	2.83	2.95	2.48	4.04	4.25	1.51	1.47	1.49	1.34	1.11	1.13	1.10	1.94	1.96	2.82
		Median	1.76	1.81	1.66	0.91	0.91	1.01	2.25	2.33	2.27	2.62	2.66	2.82	3.15	3.38	1.48	1.40	1.47	1.33	1.08	1.10	0.95	1.81	1.84	2.05
	Background (mg kg^{-1})		4.13			0.020			11.60			6.04			0.008			24.00			9/79			44.60		
East China Sea	Shanghai	Year	10	5	9	24	22	10	22	19	9	25	23	10	11	6	9	23	19	6	25	23	10	24	22	9
		Mean	2.35	2.71	2.27	7.87	9.05	7.05	6.35	6.70	5.51	4.00	4.01	3.88	6.70	8.41	5.82	1.14	1.06	1.48	2.07	1.96	2.46	1.67	1.70	1.73
		Median	2.35	2.45	2.28	8.05	8.20	6.86	6.52	6.80	6.09	3.38	3.02	3.84	6.74	8.50	6.25	0.94	0.91	1.41	2.16	1.51	2.44	1.52	1.47	1.73
	Zhejiang	Year	16	14	9	20	18	12	15	13	10	20	18	13	19	16	10	11	7	7	29	18	22	19	17	13
		Mean	2.44	2.49	2.83	7.46	8.82	6.07	5.81	5.46	6.21	4.97	5.07	4.53	10.99	12.00	6.33	1.56	1.55	1.62	3.23	2.68	3.38	2.05	1.94	2.10
		Median	2.55	2.42	2.66	7.03	7.69	6.02	5.23	5.01	6.53	5.04	5.05	5.07	6.63	6.65	5.81	1.66	1.58	1.80	3.03	2.60	3.20	2.10	2.01	2.30
	Fujian	Year	15	15	2	22	22	3	14	13	3	23	23	5	17	17	2	13	12	3	22	22	5	21	21	5
		Mean	2.26	2.28	2.20	10.49	11.62	3.47	4.78	4.20	6.92	4.62	4.92	3.66	8.60	8.44	9.47	1.42	1.34	1.63	4.34	4.50	3.42	2.93	3.05	2.85
		Median	2.26	2.32	2.20	7.98	9.19	3.42	4.31	4.11	5.94	4.19	4.44	3.36	8.41	8.41	9.47	1.38	1.28	1.55	4.31	4.45	3.63	2.51	2.51	2.21
	Background (mg kg^{-1})		4.17			0.070			23.50			4.75			0.023			24.00			13.10			44.00		
South China Sea	Guang-dong	Year	38	38	28	39	39	28	39	39	28	39	39	28	37	36	26	39	39	24	39	39	28	39	39	28
		Mean	3.72	4.24	1.71	9.61	10.43	2.05	3.23	3.67	1.11	10.02	10.78	3.38	5.16	5.40	3.09	1.51	1.69	0.54	3.10	3.34	1.94	2.71	2.88	1.59
		Median	3.75	4.52	1.18	8.52	10.39	0.39	3.22	3.81	0.87	8.28	9.18	2.25	3.48	3.68	3.13	1.47	1.69	0.53	2.98	3.21	1.93	2.58	2.82	1.49
	Guangxi	Year	32	32	5	32	32	5	9	9	3	32	32	4	32	32	5	2	2	nd[#]	32	32	5	30	30	3
		Mean	1.94	1.92	2.09	2.20	2.34	1.87	1.49	1.47	1.93	2.91	2.95	4.93	3.69	3.73	2.53	0.77	0.77	nd	1.68	1.68	2.03	1.05	1.05	1.29
		Median	1.84	1.76	1.88	1.81	1.82	1.71	1.42	1.42	1.89	2.92	2.92	2.81	2.75	2.75	2.61	0.77	0.77	nd	1.79	1.78	2.40	0.93	0.91	1.19
	Hainan	Year	10	9	3	12	12	3	9	8	3	12	12	3	11	9	3	4	3	2	12	12	3	12	12	3
		Mean	1.93	2.02	2.06	5.08	5.29	3.14	1.82	2.00	1.34	3.56	4.16	2.16	2.54	2.08	3.68	0.75	1.01	0.53	2.00	2.03	1.50	1.53	1.59	1.14
		Median	2.08	2.23	2.28	2.40	3.73	1.70	1.71	1.98	1.44	3.29	3.94	1.92	1.74	1.74	1.30	0.65	1.24	0.53	2.05	2.05	1.74	1.59	1.59	1.35
Bohai Sea	Liaoning			B*	AB		C	BC		EF	BC		B	B		AB	D		ABCD	CDE		DE	CDE		AB	B
	Hebei			B	B		C	C		EF	BC		B	B		AB	D		ABCD	ABCD		DE	DE		CDE	BC
	Tianjin			B	AB		C	C		D	B		B	AB		B	D		AB	AB		D	CDE		A	A
Yellow Sea	Shandong			B	B		C	C		E	BC		B	AB		AB	CD		D	BCD		E	E		EF	BC
	Jiangsu			B	AB		C	BC		EF	BC		B	AB		B	D		AB	ABC		E	DE		E	B
East China Sea	Shanghai			B	AB		AB	A		A	A		B	AB		AB	ABC		CD	AB		D	BC		E	BC
	Zhejiang			B	A		AB	AB		B	A		B	A		A	AB		ABC	A		C	A		DE	BC
	Fujian			B	AB		A	ABC		C	A		B	AB		AB	A		ABC	AB		A	AB		BC	B
South China Sea	Guangdong			A	B		A	C		CD	C		A	AB		AB	D		A	E		B	CD		BCD	C
	Guangxi			B	AB		C	BC		F	BC		B	AB		B	D		BCD	nd		D	CDE		F	BC
	Hainan			B	AB		BC	ABC		EF	BC		B	AB		B	BCD		ABCD	DE		CD	CDE		EF	BC

[¶]Provinces were listed from north to south along the coast of China mainland.
[§]Background values of the selected metals in the four marine zones were derived from Ji (2011) for according provinces and the background value of Ni was from Zhao and Yan (1993) for the whole coast of China.
[η]Data less than 1 were in red.
[#]"nd" was abbreviated from "no data".
*Different letters indicate differences among the 11 provinces at a significance level at $p < 0.05$, explored by One-Way ANOVA with a Tukey's multi-comparison method, and NS represents "not significant" with yearly data as the replicates.

Table 3
Status of metal loads in nearshore sediment along the coast of China mainland in the period 1980–2020.

Province	Item	As	Cd	Cr	Cu	Hg	Ni	Pb	Zn
Liaoning	Number[a]	8	11	9	12	9	2	12	1
	China-Class I[b]	1[d]	1	1	0	1		0	1
	NOAA-ERL[c]	5	0	1	0	2	2	1	1
Hebei	Number	2	9	6	9	7	2	9	9
	China-Class I	0	3	0	0	1		0	0
	NOAA-ERL	1	0	0	0	1	2	0	0
Tianjin	Number	19	27	20	27	19	25	27	27
	China-Class I	2	2	2	7	3		0	0
	NOAA-ERL	18	0	2	8	3	25	1	0
	NOAA-ERM	0	0	0	0	0	1	0	0
Shandong	Number	18	33	19	33	27	28	33	33
	China-Class I	1	2	1	1	1		0	0
	NOAA-ERL	13	0	1	1	2	11	1	0
Jiangsu	Number	38	37	38	38	37	37	38	38
	China-Class I	2	5	6	3	1		0	1
	NOAA-ERL	32	0	4	4	2	36	0	1
	NOAA-ERM	0	0	0	0	0	2	0	0
Shanghai	Number	5	22	19	23	6	19	23	22
	China-Class I	0	1	8	3	0		0	1
	NOAA-ERL	5	0	8	3	0	14	0	1
Zhejiang	Number	14	18	13	18	16	7	18	17
	China-Class I	0	0	1	4	1		0	0
	China-Class II	0	0	0	0	1		0	0
	NOAA-ERL	11	0	1	5	1	7	0	0
	NOAA-ERM	0	0	0	0	1	0	0	0
Fujian	Number	15	22	13	23	17	12	22	21
	China-Class I	0	2	0	5	0		3	4
	NOAA-ERL	11	0	0	5	0	11	8	4
	NOAA-ERM	0	0	0	0	0	1	0	0
Guangdong	Number	38	39	39	39	36	39	39	39
	China-Class I	15	28	26	27	5		0	6
	China-Class II	0	2	1	1	1		0	0
	China-Class III	0	0	0	1	0		0	0
	NOAA-ERL	35	3	26	28	9	39	13	6
	NOAA-ERM	0	0	0	1	0	3	0	0
Guangxi	Number	32	32	9	32	32	2	32	30
	China-Class I	0	1	0	0	0		0	0
	NOAA-ERL	14	0	0	0	0	1	0	0
Hainan	Number	9	12	8	12	9	3	12	12
	China-Class I	0	2	0	0	0		0	0
	China-Class II	0	1	0	0	0		0	0
	NOAA-ERL	5	1	0	0	0	2	0	0
Thresholds ($mg\ kg^{-1}$)	China-Class I	20	0.5	80	35	0.20	–	60	150
	China-Class II	65	1.5	150	100	0.50	–	130	350
	China-Class III	93	5.0	270	200	1.00	–	250	600
	NOAA-ERL	8.2	1.2	81	34	0.15	20.9	46.7	150
	NOAA-ERM	70	9.6	370	270	0.71	51.6	218	410

[a] Number refers to the number of years in 1980–2020 with C_w records.
[b] China SQGs refers to the environmental quality guidelines for marine sediment issued by China Mainland Administration as GB18668-2002, which classifies into Class I, II, and III.
[c] NOAA refers to the National Oceanic and Atmospheric Administration of USA, and ERL is abbreviated from "Effect Range Low" and ERM from "Effect Range Medium".
[d] The digit indicates the number of yearly C_w records exceeding the threshold.

ΣHQ for both SQGs and Hebei and Guangxi were significantly fitted only against US NOAA SQGs ($p < 0.05$, Fig. 3). No more significant fittings were observed in the rest provinces. On the other hand, the EKC fittings between ΣHQ to urban population percentile did not show consecutive patterns which depended on the urban population percentile change of individual provinces (Fig. 4). ΣHQ of both SQGs were similar to urban population percentile changes of the provinces in the period 1980–2020 with no significant fittings.

4. Discussion

Anthropogenic increments of metal loads in coastal sediment were evident due to various anthropogenic activities emitting metals. Metal mining and smelting activities were commonly considered as the primary sources for most metal loads in sediment. A 4500-year sediment core from the Italian coast recorded a sudden strong enrichment due to mining with industrialization in the 19th century (Bergamin et al., 2021). Another 3500-year Mediterranean sediment core explored that Pb loads in sediment exponentially increased from the end of the 19th century and coal combustion was the predominant Pb source (Elbaz-Poulichet et al., 2011). However, some arguments remained to decipher mining impacts or high geochemical backgrounds (natural weathering) for metal loads in coastal sediment, such as in estuaries of Chilean rivers (Viers et al., 2019) and Yangtze River (Guo and Yang, 2016). Evidence from isotope analyses indicated that sedimentary Cu and Zn were dominated by urban sources after smelter closed in the 1980s in Seattle region, USA (Thapalia et al., 2010). Urban regions have significant metal loads in sediment from various sources, for instance, coal combustion and vehicular exhausts (Li et al., 2012a, 2012b, 2013; Ma et al., 2016). This study found that nearshore sediment of all the 11 coastal provinces in China mainland had considerable anthropogenic metal loads in the period 1980–2020 (Table 2). According to the National Bureau of Statistics, China (data.stats.gov.cn), Guangdong emitted the greatest amounts of Pb (4947 kg), Hg (61 kg), and Cd (520 kg) via wastewater discharge in 2020 while Zhejiang and Shandong led the discharges of Cr (2961 kg with 849 kg as Cr VI) and As (653 kg), respectively (Table 5). It is coincident to the findings of this study, i.e., Guangdong with the highest mean C_w of Pb, Hg, and Cd loads in nearshore sediment among the 11 coastal provinces in the period 1980–2020 but Hg not significantly ($p < 0.05$, Table 1). However, Guangdong also had the greatest mean C_w of As and Cr loads in nearshore sediment and were significantly higher than Zhejiang and Shandong, respectively, in the period 1980–2020 ($p < 0.05$, Table 1).

As hypothesized, the spatiotemporal and element differences of metal loads in nearshore sediment among the 11 provinces would be associated with their various levels of industrialization and urbanization (Figs. 2, 3, and 4, and Table 4). It is well-known that plating and electroplating, and leather tannery are two industries which discharge considerable metals in the wastes (Fu and Wang, 2011; Yuan et al., 2016). As the Report of market forward and investment strategy planning on China plating industry (2022–2027) (https://bg.qianzhan.com/report/detail/8fda9e11cacd4df2.html) summarized, Guangdong has 20 plating industrial parks, followed by Jiangsu (8 parks), Zhejiang (5 parks), Liaoning and Shandong (3 parks each), Fujian, Hebei and Tianjin (1 park each); among the plating metals, Zn plating has 45–50% of market share, Cu, Ni, and Cr about 30% share, anode treatment about 15% share, and Pb/Tin and Au about 5% share in China mainland; but utilization rates are about 65%, 75%, and 10.5% for Cu, Ni, and Cr plating, respectively. Accordingly, electroplating and plating related metals would contribute their loads in coastal sediment. Similarly, leather tannery is also highly distributed in the coastal provinces, including Hebei (123.7 million m^2), Zhejiang (63.6 million m^2), Guangdong (33.2 million m^2), Jiangsu (19.6 million m^2), Shandong (16.9 million m^2), and Fujian (14.1 million m^2), all ranking in top 10 of light leather production in the first half year of 2017 (https://www.askci.com/news/chanye/20180404/171058121022.shtml). Obviously, the distribution of electroplating and plating, and leather tannery in the coastal provinces might explain the partial loads of these industry-related metals in nearshore sediment.

Energy combustion is another important source of metal emission (Le Roux et al., 2016). Especially, Chinese coals are enriched with various metals, including Pb (Fang et al., 2014), As (Kang et al., 2011), and Hg and others (Ren et al., 1999). Coincidently, Shandong consumed the greatest volume (431.3 million tons) of coal in 2019 and emitted 796 kg Pb (No. 3) and 653 kg As (No. 1) among the 11 coastal provinces while Hainan, Shanghai, and Tianjin used the lowest volumes of coal and also emitted the lowest amounts of Pb and As accordingly (Table 5). The coincidences might be confirmed by multiple sediment cores from Shanghai parks, over 50% of Pb load in sediment derived from coal combustion (Li et al., 2012a). However, in the period 1980–2020 the nearshore sediment had the mean yearly loads (C_w) of Pb and As in Shandong not significantly different to Hainan and Shanghai, and even had Pb loads significantly

Table 4
Interactions between anthropogenic increment rate ($R_{anthrop}$) of the selected metal loads in coastal sediment and provincial socioeconomics in China mainland in the period 1980–2020 explored by canonical redundancy analysis.

Province		Liaoning	Hebei	Tianjin	Shandong	Jiangsu	Shanghai	Zhejiang	Fujian	Guangdong	Guangxi	Hainan	Nation				
Number of metals[¶]		4	4	8	6	8	6	7	7	8	6	4	8	7	6	5	4
Yearly record		11	9	18	22	37	18	12	12	36	30	12	121	153	179	213	256
R^2		0.6510	0.9725	0.9527	0.8622	0.5418	0.9275	0.9888	0.9385	0.5081	0.6469	0.5006	0.3624	0.2917	0.2200	0.2132	0.1727
Canonical variables of socioeconomics																	
Self-explanation (%)		1.35	59.59	12.71	30.63	79.85	62.01	13.64	17.86	94.83	77.56	3.97	9.77	11.85	12.28	15.47	25.54
Opposite-explanation (%)		0.88	57.95	12.11	26.41	43.26	57.51	13.49	16.76	48.19	50.17	1.99	3.55	3.46	2.70	3.30	4.41
Square multi-correlations to the 1st M canonical variables of Metals	Urban population (%)	0.0168	0.6112	0.0006	0.2654	0.4514	0.9153	0.0705	0.2474	0.4112	0.5063	0.0433	0.0013	0.0951	0.1037	0.1168	0.1205
	GDP per capita	0.0038	0.5415	0.1419	0.2284	0.4243	0.5272	0.1902	0.1365	0.5070	0.4986	0.0126	0.0677	0.0218	0.0039	0.0103	0.0387
	AGDP per capita	0.0145	0.5298	0.1261	0.2422	0.4004	0.5317	0.1178	0.1322	0.5043	0.4785	0.0114	0.0289	0.0182	0.0000	0.0013	0.0007
	NAGDP per capita	0.0002	0.6352	0.2158	0.3205	0.4544	0.3262	0.1609	0.1545	0.5049	0.5235	0.0123	0.0437	0.0033	0.0004	0.0036	0.0166
Canonical variables of metals																	
Self-explanation (%)		40.89	30.24	33.11	15.22	7.81	27.79	21.01	19.85	9.78	19.36	6.60	9.96	20.67	21.79	27.56	33.35
Opposite-explanation (%)		26.62	29.41	31.55	13.12	4.23	25.78	20.77	18.62	4.97	12.52	3.30	3.61	6.03	4.79	5.88	5.76
Square multi-correlations to the 1st M canonical variables of socioeconomics	As	Excluded	Excluded	0.2750	Excluded	0.0224	Excluded	0.3824	0.0073	0.2183	0.2135	Excluded	0.0000	0.0039	0.0112	Excluded	Excluded
	Cd	0.2205	0.8432	0.0909	0.1389	0.0130	0.2882	0.0453	0.1084	0.0165	0.0001	0.0301	0.0208	0.0641	0.0363	0.0442	0.0593
	Cr	Excluded	Excluded	0.2786	Excluded	0.0441	0.0797	0.1618	0.3840	0.0680	Excluded	Excluded	0.0431	0.1542	Excluded	Excluded	Excluded
	Cu	0.5492	0.1752	0.0635	0.0247	0.0550	0.1133	0.4209	0.3102	0.0268	0.2304	0.0386	0.0019	0.0042	0.0019	0.0045	0.0034
	Hg	Excluded	Excluded	0.0547	0.1068	0.0573	Excluded	0.3387	0.1430	0.0283	0.0280	Excluded	0.0821	0.0244	0.0025	0.0005	Excluded
	Ni	Excluded	Excluded	0.7944	0.1201	0.0159	0.5548	Excluded	Excluded	0.0331	Excluded	Excluded	0.0476	Excluded	Excluded	Excluded	Excluded
	Pb	0.1435	0.1149	0.2387	0.2167	0.1187	0.3079	0.0788	0.0406	0.0000	0.0077	0.0617	0.0096	0.0273	0.0543	0.0589	0.0398
	Zn	0.1516	0.0431	0.7280	0.1803	0.0122	0.2028	0.0360	0.3103	0.0064	0.2716	0.0018	0.0837	0.1440	0.1813	0.1856	0.1279

[¶] The metals with the number of yearly records less than the number of variables (4 socioeconomic indicators + the selected metals) were omitted according to the requirement of Canonical Redundancy Analysis.

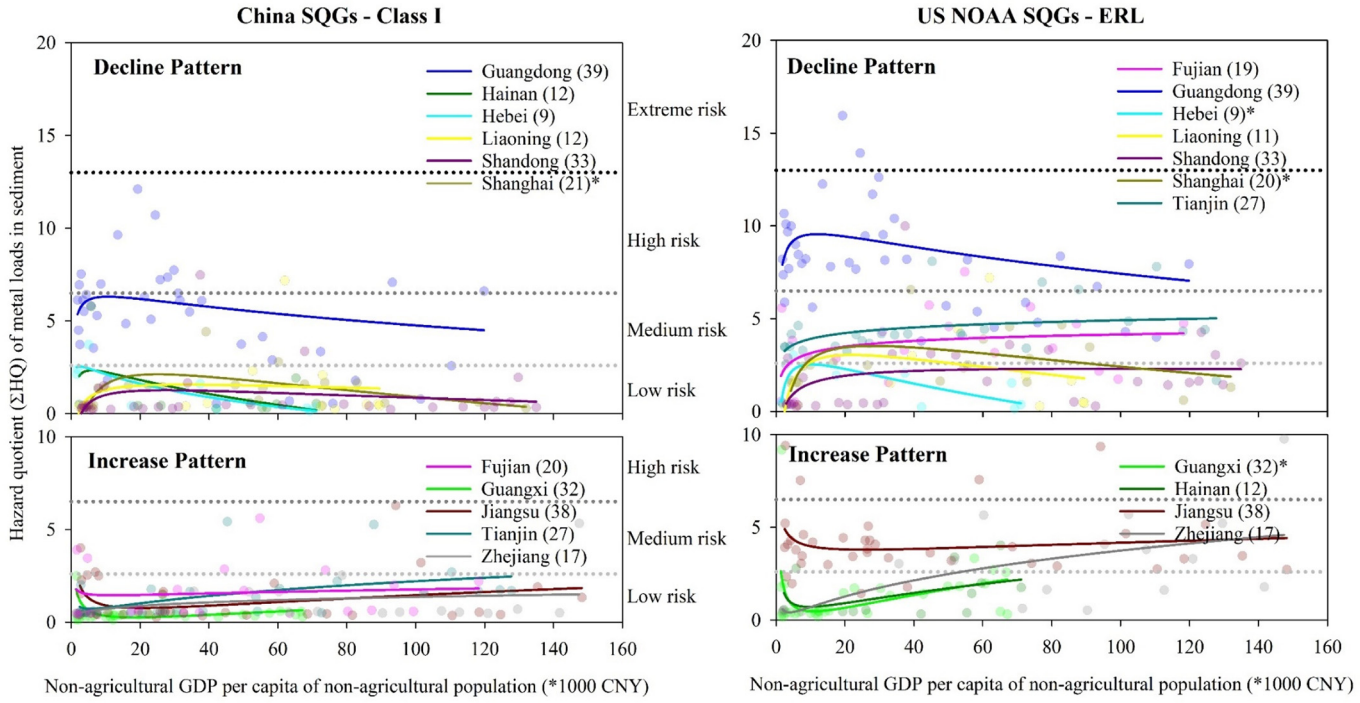

Fig. 3. Provincial patterns of hazard quotient (ΣHQ) of metal loads in nearshore sediment in relation to non-agricultural GDP per capita of non-agricultural population (NAGDP per capita) simulated by the Environmental Kuznets Curve (EKC) model. Two sediment quality guidelines (SQGs) were employed as China SQGs (GB18668-2002, Class I without Ni threshold) and US NOAA SQGs (ERL, effect range low). Risks of metal loads in sediment were classified into low risk (ΣHQ ≤ 2.6), medium risk (2.6 < ΣHQ ≤ 6.5), high risk (6.5 < ΣHQ ≤ 13), and extreme risk (ΣHQ > 13). The ΣHQ by China SQGs - Class I included at least 4 metals out of As, Cd, Cr, Cu, Hg, Pb, and Zn, and the one by US NOAA SQGs - ERL included at least 5 metals out of As, Cd, Cr, Cu, Hg, Ni, Pb, and Zn. The number in parentheses after provinces in the legend was the number of the years in the period 1980–2020 involved for the ΣHQ calculations. Significant EKC fitting ($p < 0.05$) was labeled with "*" after the province in the legend.

lower than those in Tianjin ($p < 0.05$, Table 1). It is possibly due to Shanghai (61.43 million tons in 2011) and Tianjin (52.98 million tons in 2012) dramatically reducing coal consumption in the past decade over 40% of the peak amount but Shandong (389.21 million tons in 2011) increasing more than 10% amount (data.stats.gov.cn). On the other hand, vehicular metal emission is also an important anthropogenic source (Le Roux et al., 2016), for instance, vehicular Pb contributing approximately 10% of Pb load in sediment of Shanghai parks (Li et al., 2012a) and significantly increasing sedimentary Pb levels in the Hangzhou Xixi National Wetland Park in three years (Ma et al., 2016). Some emerging industries, such as e-waste recycling, resulted in considerable metal emissions in Guangdong and Zhejiang (Song and Li, 2014).

The above argued interactions between metal loads in coastal sediment and mainstream of economic development (indicated by NAGDP per capita) in the coastal provinces by the EKC model fitting in this study suggested that two possible patterns existed in the period 1980–2020, i.e., metal emission decline (inversed U shape) or increase (U shape) with the economic development (Fig. 3). Only 3 provinces shifted with the two SQGs, maybe due to Ni contamination (US NOAA SGQs has Ni thresholds and China SQGs does not). The two EKC patterns were observed by other studies to fit economic indicator with CO_2 emission, air quality, or statistical pollutant emissions (Capps et al., 2016; Chen and Xu, 2017; Wang et al., 2017). The inversed U shape (decline pattern) hints that these provinces stepped on the low impact development of metal emissions while the U

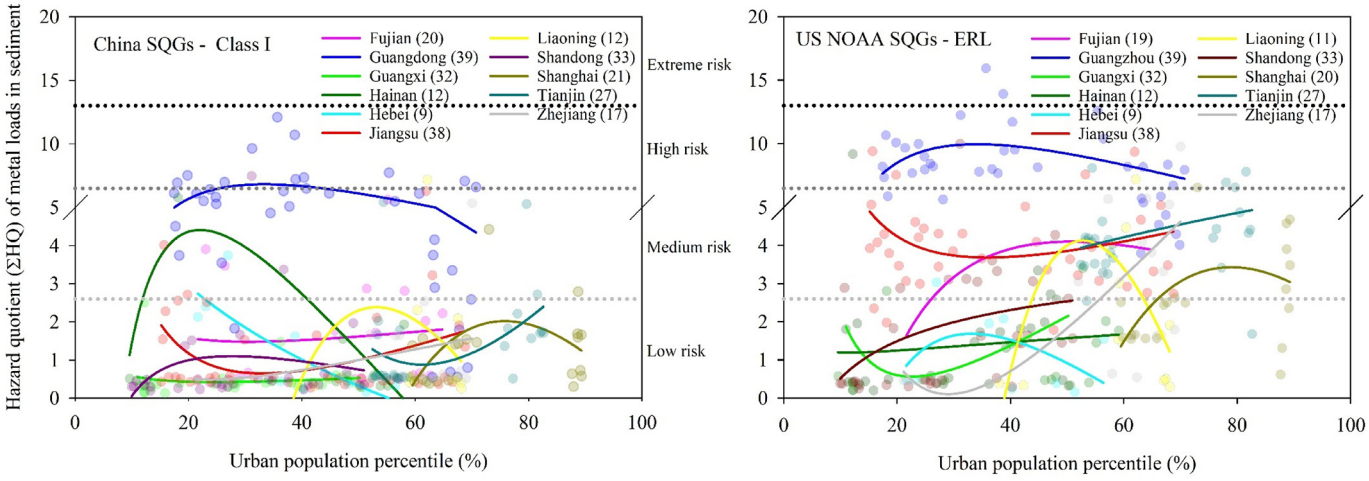

Fig. 4. Provincial patterns of hazard quotient (ΣHQ) of metal loads in nearshore sediment in relation to urban population percentile simulated by the Environmental Kuznets Curve (EKC) model. Detailed information refers to Fig. 3.

Table 5
Selected socioeconomic indicators in 2019 and metal emissions via wastewater discharges in 2020 according to the National Bureau of Statistics, China (data.stats.gov.cn).

Province[¶]	Socioeconomic indicators in 2019 before the COVID-19 pandemic								Metal emission via wastewater discharge in 2020					
	GDP[§] (billion CNY)	AGDP (billion CNY)	NAGDP (billion CNY)	Industrial GDP (billion CNY)	GDP per capita (CNY)	AGDP per capita (CNY)	NAGDP per capita (CNY)	Coal consumption (million ton)	Pb (kg)	Hg (kg)	Cd (kg)	Cr (kg)	As (kg)	Cr_{VI} (kg)
Liaoning	2486	218	2268	805	58,019	17,693	74,449	187.1	44	17	7	269	112	46
Tianjin	1406	19	1387	437	101,557	8544	118,751	37.7	23	5	3	125	20	32
Hebei	3498	35	3463	1131	47,036	1146	79,111	287.4	70	6	2	670	65	70
Shandong	7054	512	6542	2276	69,901	13,277	104,644	431.3	796	36	146	2664	653	255
Jiangsu	9866	430	9436	3723	116,650	18,427	153,755	249.0	312	29	10	2115	103	474
Shanghai	3799	11	3788	957	153,299	4034	171,093	42.4	58	3	15	197	47	48
Zhejiang	6246	209	6038	2252	98,770	11,516	132,315	136.8	409	7	90	2961	56	849
Fujian	4233	260	3973	1565	102,722	19,530	141,493	87.2	500	20	91	976	208	117
Guangdong	10,799	435	10,364	3914	86,956	12,736	114,225	168.3	4947	61	520	2330	444	602
Guangxi	2124	339	1785	525	42,778	14,467	67,629	80.2	848	30	252	253	350	45
Hainan	533	108	425	60	53,929	26,708	71,942	11.3	10	0	4	39	11	9

[¶] Provinces were listed from north to south along the coast of China mainland.
[§] GDP is abbreviated from gross domestic product; AGDP refers to agricultural GDP; NAGDP refers to non-agricultural GDP, a difference between GDP and AGDP.

shape (increase pattern) suggests more metal emissions during the development, such as manufacturing holding or high energy consumption provinces (Zhejiang and Jiangsu) or rapidly developing province (Guangxi and Hainan) (Fig. 3; Destek and Sarkodie, 2019; Sarkodie and Strezov, 2019; Zhou et al., 2019). Overall, the EKC model fittings were only significant in Shanghai for both SQGs (decline pattern), and Hebei (decline pattern) and Guangxi (increase pattern) only for US NOAA SQGs (Fig. 3). Integrating the results of canonical redundancy analysis and the EKC model fitting, it suggests that a better explanation or coupling requires to decouple socioeconomic sectors (i.e., NAGDP per capita) finely and to identify metal-emission related sectors, like CO_2 emission sectors done by Congregado et al. (2016). However, urban population percentile (urbanization indicator) might be inappropriate as a socioeconomic indictor for exploring the interactions between environmental quality change and urbanization among multiple regions under various urbanization levels (Fig. 4). No significant EKC model fittings existed for the two SQGs among the 11 provinces. It might be because urban population percentile is not an indicator with consecutive or linearly relationships to metal emission from manufacturing, which is determined by production, and maybe better for metal emissions from consumptions by regional population.

Although spatiotemporal variations of metal loads in nearshore sediment among the 11 coastal provinces of China mainland in the period 1980–2020, metal pollutions were not serious as imagined. Most exceeders of metal loads in nearshore sediment were found at the lowest or best thresholds of China SQGs - Class I or US NOAA SQGs ERL (Table 4) although Guangdong had the medium-to-high risk (Class I) or high-to-extreme risk (ERL) (Fig. 3). In comparison to metal loads in coastal sediment, nearshore sediment of China mainland in 1980–2020 was relatively higher than the southern coast in Korea (Hwang et al., 2019), the western Gulf of Thailand (Liu et al., 2016), the Noakhali coast in Bangladesh (Siddique et al., 2021), Pacific coast in Palau (Jeong et al., 2021), and Gorgan Bay in Iran (Bastami et al., 2012) in Asia, and Jade Bay in Germany (Beck et al., 2013) and Black Sea coast in Turkey (Alkan et al., 2015) in Europe, and Jurujuba Sound coast in Brazil (Baptista Neto et al., 2000) and Nador lagoon in Morocco (Maanan et al., 2015) had metal loads in coastal sediment fully higher than the nearshore of China mainland in the period 1980–2020 for all the selected metals. Other coasts in literature had metal loads in coastal sediment varying with metal elements in comparison with nearshores of China mainland (Table 6).

5. Conclusions

Eight selected metal loads in nearshore sediment along the coast of China mainland were summarized via extracting data from literature in the period 1980–2020 with a sample number weighted content (C_w) transformation. Significant spatial (geographic) variations in metal loads (C_w) were presented among the 11 coastal provinces and better spatial patterns were achieved with anthropogenic increment rate ($R_{anthropo}$) calculated from yearly C_w records of each selected metal against the regional coastal sediment backgrounds. Temporal changes of the selected metals in nearshore sediment differed among the 11 provinces and could be partially explained by few key anthropogenic sources of metal emissions, such as plating and electroplating, leather tannery, and coal consumption. However, the quantitative delineations by the classic EKC model fitting were not successful as hypothesized for the interactions between metal loads in nearshore sediment and socioeconomic development although the canonical correlations were identified between the socioeconomic indicators and the metal loads ($R_{anthropo}$) in nearshore sediment provincially. This study explored that urban population percentile, a widely used indicator for urbanization, could not explain the interactions between regional urbanization and metal loads in coastal sediment. It might be because metal loads in coastal sediment were derived from both manufacturing and population consumption while urban population percentile mainly indicated anthropogenic consumption. Obviously, a large uncertainty existed for explaining interactions between metal loads in coastal sediment and socioeconomic development provincially. The uncertainty might be derived from both sides. Socioeconomic indicators might have to break down to metal emission sectors instead of general indicators although NAGDP per capita used in this study is a subsector of GDP per capita. On the other side, the collected data of metal loads in coastal sediment only had few full yearly records for all the 8 selected metals as well as considerable spatial heterogeneity in a province. A secondary uncertainty might be derived from the analytical approaches upgrading and diversity in the period 1980–2020, for instance, from AAS to ICP-A/OES and ICP-MS, AFS, and XRF. To improve the delineations of the interactions between metal loads in coastal sediment and socioeconomic development in province, undisturbed sediment cores covering 100-year history of environmental changes might be manipulatable instead of the meta-data analyses in the future coupling with metal emission related socioeconomic indicators.

Supplementary data to this article can be found online at https://doi.org/10.1016/j.scitotenv.2022.156286.

CRediT authorship contribution statement

Xun Liu: Formal analysis, Investigation, Data curation, Writing - Original Draft. **Shen Yu**: Conceptualization, Resources, Formal analysis, Data curation, Writing - Review & Editing, Visualization, Supervision, Project administration, Funding acquisition.

Table 6
Metal loads (mg kg^{-1}) in coastal sediment of China Mainland summarized in this study in comparison to the elsewhere in the world.

Continent	Location	As	Cd	Cr	Cu	Hg	Ni	Pb	Zn	Reference
Asia	Nearshore coast, China Mainland	12.8 (1.82-88.3)	0.328 (0.010-9.50)	69.3 (3.63-389)	29.0 (0.300-794)	0.095 (0.002-1.39)	34.3 (5.00-135)	31.8 (0.130-180)	92.3 (1.01-1008)	This study
	Southern coast, Korea	7.40[¶] (BDL[§]-27.4)	0.090 (BDL-1.37)		13.8 (0.180-104)	0.010 (BDL-0.240)		24.1 (0.040-85.4)	73.0 (1.00 -331)	Hwang et al., 2019
	Beppu Bay, Japan	11.6 (7.20-22.3)	0.300 (0.190-0.470)	43.8 (34.0-76.0)	33.4 (25.9-37.3)			28.5 (24.7-32.2)	129 (111-144)	Amano et al., 2011
	Dumai coast, Indonesia		0.880 (0.460-1.89)		6.08 (1.61-13.8)		11.5 (7.26-20.0)	32.3 (14.6-84.9)	53.9 (31.5-87.1)	Amin et al., 2009
	West coast of Peninsular, Malaysia	60.4 (34.1-113)	0.825 (0.280-1.55)	46.4 (30.2-74.8)	17.4 (11.4-40.6)	0.230 (0.170-0.350)	11.4 (6.20-17.83)	59.5 (47.5-85.9)	51.1 (32.8-127)	Sany et al., 2013
	Cau Hai lagoon,Vietnam	15.0 (6.00-20.0)	0.300 (0.200-0.400)	77.0 (44.0-98.0)	15.0 (8.00-20.0)		27.0 (14.0-32.0)	45.0 (23.0-53.0)	93.0 (47.0-123)	Tran et al., 2018
	Western Gulf of Thailand	3.78 (1.06-34.1)	0.090 (0.020-0.170)	50.8 (8.08-82.6)	12.3 (2.20-25.3)	0.020 (0.0-0.110)		21.4 (4.13-38.8)	45.0 (1.63-79.0)	Liu et al., 2016
	Noakhali coast, Bangladesh		0.280 (0.110-0.650)	10.6 (0.450-18.6)	6.22 (0.010-16.6)			12.5 (6.78-25.0)	42.4 (4.90-97.8)	Siddique et al., 2021
	Coramandal Coast, India		19.8 (3.30-19.8)	109 (57.8-110)			28.0 (7.40-28.0)	49.6 (2.70- 49.6)	78.8 (8.50-78.8)	Anbuselvan et al., 2018
	Pacific Ocean, Palau	12.8 (0.900-43.5)	0.018 (0.001-0.052)	61.6 (4.9-451)	8.00 (1.10-66.4)	0.015 (0.002-0.070)	14.1 (5.1-67.9)	1 (0.100-2.70)	11.0 (0.700-52.5)	Jeong et al., 2021
	Gorgan Bay, Iran			15.2 (4.10–18.3)	8.83 (3.80-31.2)			11.5 (4.10-18.3)	22.2 (13.0-75.0)	Bastami et al., 2012
Europe	Jade Bay, Germany	8.00	0.250	49.0	7.00		10.0	16.0	43.0	Beck et al., 2013
	Berre Coastal Lagoon, France		0.230 (0.200-1.40)	58.7 (17.1-119)	31.0 (7.00-60.7)			41.7 (12.0-104)	120 (56.5-215	Arienzo et al., 2013
	Campania, Italy	35.2 (12.3-100)	0.020 (0.0-0.700)	14.0 (0.500-49.5)	25.6 (3.50-86.2)	5.80 (0.0-25.3)	9.90 (0.0-35.4)	105.8 (11.5-378)	225 (42.1-870)	Trifuoggi et al., 2017
	Medway Estuary, UK	14.0		76.0	42.0		28.0	67.0	138	Spencer, 2002
	Black Sea coast of Turkey	7.10 (4.30-12.1)	0.300 (0.260-0.370)	18.5 (9.70-29.5)	31.8 (22.2-46.6)		13.8 (8.30-25.2)	22.4 (17.7-29.5)	70.2 (50.0-89.2)	Alkan et al., 2015
Americas	Nova Scotia, Canada	5.64 (0.500-62.0)	0.450 (0.050-3.80)	18.4 (1.00-305)	22.7 (0.500-220)	0.050 (0.003-1.85)	15.9 (2.00-697)	25.4 (0.730-583.0)	86.1 (5.00-2300)	Zhang et al., 2019a
	Jurujuba Sound coast, Brazil			89.0 (10.0-223)	51.0 (5.00-213)		48.0 (15.0-79.0)	61.0 (5.00-123)	158 (15.0-337)	Baptista Neto et al., 2000
Africa	Nador lagoon, Morocco		1.60 (0.120-3.60)	71.6 (22.4-172)	151 (10.2-398)		45.2 (20.2-95.2)	135 (15.6-326)	555 (55.1-1250)	Maanan et al., 2015
	Red Sea coast, Egypt		0.534 (0.120-1.25)		9.43 (3.67-17.3)		17.5 (3.43-44.1)	11.43 (3.43-44.1)	44.2 (14.9-134)	Nour et al., 2019

[¶]Data in color represented greater than mean C_w of each metal in this study in red and lower in blue.
[§]"BDL" was an abbreviation of "below detection limit".
Note: References cited for the various coasts were listed in a sequence of each row as: This study; Hwang et al., 2019; Amano et al., 2011; Amin et al., 2009; Sany et al., 2013; Tran et al., 2018; Liu et al., 2016; Siddique et al., 2021; Anbuselvan et al., 2018; Jeong et al., 2021; Bastami et al., 2012; Beck et al., 2013; Arienzo et al., 2013; Trifuoggi et al., 2017; Spencer, 2002; Alkan et al., 2015; Zhang et al., 2019a; Baptista Neto et al., 2000; Maanan et al., 2015; Nour et al., 2019.

Declaration of competing interest

The authors declare that they have no known competing financial interests or personal relationships that could have appeared to influence the work reported in this paper.

Acknowledgements

Authors appreciate helps and supports from staff in the instrument center and three anonymous reviewers. This work was supported by the National Natural Science Foundation of China [No. 41661144033, 41571483, 71961137007].

References

Alkan, N., Alkan, A., Akbas, U., Fisher, A., 2015. Metal pollution assessment in sediments of the southeastern Black Sea coast of Turkey. Soil Sediment Contam. 24, 290–305. https://doi.org/10.1080/15320383.2015.950723.

Amano, A., Kuwae, M., Agusa, T., Omori, K., Takeoka, H., Tanabe, S., Sugimoto, T., 2011. Spatial distribution and corresponding determining factors of metal concentrations in surface sediments of Beppu Bay, Southwest Japan. Mar. Environ. Res. 71, 247–256. https://doi.org/10.1016/j.marenvres.2011.01.009.

Amante, C., Eakins, B., 2009. Memorandum NESDIS NGDC-24. National Geophysical Data Center, NOAA.

Amin, B., Ismail, A., Arshad, A., Yap, C.K., Kamarudin, M.S., 2009. Anthropogenic impacts on heavy metal concentrations in the coastal sediments of Dumai,Indonesia. Environ. Monit. Assess. 148, 291–305. https://doi.org/10.1007/s10661-008-0159-z.

Anbuselvan, N., Senthil, Nathan D., Sridharan, M., 2018. Heavy metal assessment in surface sediments off Coromandel Coast of India: implication on marine pollution. Mar. Pollut. Bull. 131, 712–726. https://doi.org/10.1016/j.marpolbul.2018.04.074.

Arienzo, M., Masuccio, A.A., Ferrara, L., 2013. Evaluation of sediment contamination by heavy metals, organochlorinated pesticides, and polycyclic aromatic hydrocarbons in the Berre Coastal Lagoon (Southeast France). Arch. Environ. Contam. Toxicol. 65, 396–406. https://doi.org/10.1007/s00244-013-9915-3.

Baptista Neto, J.A., Smith, B.J., McAllister, J.J., 2000. Heavy metal concentrations in surface sediments in a nearshore environment, Jurujuba Sound, Southeast Brazil. Environ. Pollut. 109, 1–9. https://doi.org/10.1016/S0269-7491(99)00233-X.

Bastami, K.D., Bagheri, H., Haghparast, S., Soltani, F., Hamzehpoor, A., Bastami, M.D., 2012. Geochemical and geo-statistical assessment of selected heavy metals in the surface sediments of the Gorgan Bay,Iran. Mar. Pollut. Bull. 64, 2877–2884. https://doi.org/10.1016/j.marpolbul.2012.08.015.

Beck, M., Böning, P., Schückel, U., Stiehl, T., Schnetger, B., Rullkötter, J., Brumsack, H.-J., 2013. Consistent assessment of trace metal contamination in surface sediments and suspended particulate matter: a case study from the Jade Bay in NW Germany. Mar. Pollut. Bull. 70, 100–111. https://doi.org/10.1016/j.marpolbul.2013.02.017.

Bergamin, L., Pierfranceschi, G., Romano, E., 2021. Anthropogenic impact due to mining from a sedimentary record of a marine coastal zone (SW Sardinia, Italy). Mar. Micropaleontol. 169, 102036. https://doi.org/10.1016/j.marmicro.2021.102036.

Cao, L., Hong, G.H., Liu, S., 2015. Metal elements in the bottom sediments of the Changjiang Estuary and its adjacent continental shelf of the East China Sea. Mar. Pollut. Bull. 95, 458–468. https://doi.org/10.1016/j.marpolbul.2015.03.013.

Capps, K.A., Bentsen, C.N., Ramírez, A., 2016. Poverty, urbanization, and environmental degradation: urban streams in the developing world. Freshw. Sci. 35, 429–435. https://doi.org/10.1086/684945.

Chen, N., Xu, L., 2017. Relationship between air quality and economic development in the provincial capital cities of China. Environ. Sci. Pollut. Res. 24, 2928–2935. https://doi.org/10.1007/s11356-016-8065-3.

Chen, Q., Taylor, D., 2020. Economic development and pollution emissions in Singapore: evidence in support of the environmental kuznets curve hypothesis and its implications for regional sustainability. J. Clean. Prod. 243, 118637. https://doi.org/10.1016/j.jclepro.2019.118637.

Cheung, K.C., Poon, B.H.T., Lan, C.Y., Wong, M.H., 2003. Assessment of metal and nutrient concentrations in river water and sediment collected from the cities in the Pearl River Delta, South China. Chemosphere 52, 1431–1440. https://doi.org/10.1016/s0045-6535(03)00479-x.

Congregado, E., Feria-Gallardo, J., Colpe, A.A., Iglesias, J., 2016. The environmental Kuznets curve and CO2 emissions in the USA. Environ. Sci. Pollut. Res. 233, 18407–18420. https://doi.org/10.1007/s11356-016-6982-9.

Destek, M.A., Sarkodie, S.A., 2019. Investigation of environmental Kuznets curve for ecological footprint: the role of energy and financial development. Sci. Total Environ. 650, 2483–2489. https://doi.org/10.1016/j.scitotenv.2018.10.017.

Duan, X., Zhang, G., Rong, L., Fang, H., He, D., Feng, D., 2015. Spatial distribution and environmental factors of catchment-scale soil heavy metal contamination in the dry-hot valley of Upper Red River in southwestern China. Catena 135, 59–69. https://doi.org/10.1016/j.catena.2015.07.006.

Editorial Board of Comprehensive Investigation and Assessment in Offshores of China, 2012. Provincial General Reports of Comprehensive Investigation and Assessment in Offshores. China Ocean Press, Beijing.

Editorial Board of National Comprehensive Survey of Island Resources, 1996. Report of comprehensive survey of island resources in China. China Ocean Press, Beijing.

Elbaz-Poulichet, F., Dezileau, L., Freydier, R., Cossa, D., Sabatier, P., 2011. A 3500-year record of Hg and Pb contamination in a Mediterranean sedimentary archive (the Pierre Blanche Lagoon, France). Environ. Sci. Technol. 45, 8642–8647. https://doi.org/10.1021/es2004599.

Fang, T., Liu, G.J., Zhou, C.C., Sun, R.Y., Chen, J., Wu, D., 2014. Lead in Chinese coals: distribution, modes of occurrence, and environmental effects. Environ. Geochem. Health 36, 563–581. https://doi.org/10.1007/s10653-013-9581-4.

Fang, T.H., Lien, C.Y., 2020. Mini review of trace metal contamination status in East China Sea sediment. Mar. Pollut. Bull. 152, 110874. https://doi.org/10.1016/j.marpolbul.2019.110874.

Feng, H., Jiang, H., Gao, W., Weinstein, M.P., Zhang, Q., Zhang, W., Yu, L., Yuan, D., Tao, J., 2011. Metal contamination in sediments of the western Bohai Bay and adjacent estuaries,China. J. Environ. Manag. 92, 1185–1197. https://doi.org/10.1016/j.jenvman.2010.11.020.

Fu, F., Wang, Q., 2011. Removal of heavy metal ions from wastewaters: a review. J. Environ. Manag. 92, 407–418. https://doi.org/10.1016/j.jenvman.2010.11.011.

Gao, X.L., Zhou, F.X., Chen, C.T.A., 2014. Pollution status of the Bohai Sea: an overview of the environmental quality assessment related trace metals. Environ. Int. 62, 12–30. https://doi.org/10.1016/j.envint.2013.09.019.

General Administration of Quality Supervision and Quarantine of China, I., 2002. Marine Sediment Quality Guidelines of China GB18668-2002.

Gergel, S.E., Bennett, E.M., Greenfield, B.K., King, S., Overdevest, C.A., Stumborg, B., 2004. A test of the environmental Kuznets curve using long-term watershed inputs. Ecol. Appl. 14, 555–570. https://doi.org/10.1890/02-5381.

Guo, Y., Yang, S., 2016. Heavy metal enrichments in the Changjiang (Yangtze River) catchment and on the inner shelf of the East China Sea over the last 150 years. Sci. Total Environ. 543, 105–115. https://doi.org/10.1016/j.scitotenv.2015.11.012.

Han, L., Gao, B., Hao, H., Lu, J., Xu, D., 2019. Arsenic pollution of sediments in China: an assessment by geochemical baseline. Sci. Total Environ. 651, 1983–1991. https://doi.org/10.1016/j.scitotenv.2018.09.381.

He, Q., Bertness, M.D., Bruno, J.F., Li, B., Chen, G.Q., Coverdale, T.C., Altieri, A.H., Bai, J.H., Sun, T., Pennings, S.C., Liu, J.G., Ehrkich, P.R., Cui, B.S., 2014. Economic development and coastal ecosystem change in China. Sci. Rep. 4, 5995. https://doi.org/10.1038/srep05995.

Heilig, G.K., 2006. Many Chinas? The economic diversity of China's provinces. Popul. Dev. Rev. 32, 147–161. https://doi.org/10.1111/j.1728-4457.2006.00109.x.

Hong, B., Zhou, M., Li, J., Yu, S., Xu, B., Liu, X., Chen, P., Zhou, T., Chen, Y., 2021. Legacy organochlorines in estuarine sediment in relation to socioeconomic pattern in multi-coastal watersheds. Environ. Sci. Pollut. Res. https://doi.org/10.1007/s11356-021-17350-4.

Hwang, D.W., Kim, P.J., Kim, S.G., Sun, C.I., Koh, B.S., Ryu, S.O., Kim, T.H., 2019. Spatial distribution and pollution assessment of metals in intertidal sediments, Korea. Environ. Sci. Pollut. Res. 26, 19379–19388. https://doi.org/10.1007/s11356-019-05177-z.

Jeong, H., Choi, J.Y., Choi, D.-H., Noh, J.-H., Ra, K., 2021. Heavy metal pollution assessment in coastal sediment and bioaccumulation on seagrass (Enhalus acoroides) of Palau. Mar. Pollut. Bull. 163, 111912. https://doi.org/10.1016/j.marpolbul.2020.111912.

Ji, W., 2011. Study on the current situation and background value of offshore marine environmental quality in China. China Ocean Press, Beijing, p. 304.

Kang, Y., Liu, G.J., Chou, C.L., Wong, M.H., Zheng, L.G., Ding, R., 2011. Arsenic in Chinese coals: distribution, modes of occurrence, and environmental effects. Sci. Total Environ. 412–413, 1–13. https://doi.org/10.1016/j.scitotenv.2011.10.026.

Kim, Y., Tanaka, K., Ge, C., 2018. Estimating the provincial environmental Kuznets curve in China: a geographically weighted regression approach. Stoch. Env. Res. Risk A. 32, 2147–2163. https://doi.org/10.1007/s00477-017-1503-z.

Le Roux, G., Hansson, S.V., Claustres, A., 2016. Chapter 3 - inorganic chemistry in the mountain critical zone: are the mountain water towers of contemporary society under threat by trace contaminants? In: Greenwood, G.B., Shroder, J.F. (Eds.), Developments in Earth Surface Processes. 21, pp. 131–154

Li, H.B., Yu, S., Li, G.L., Deng, H., 2012a. Lead contamination and source in Shanghai in the past century using dated sediment cores from urban park lakes. Chemosphere 88, 1161–1169. https://doi.org/10.1016/j.chemosphere.2012.03.061.

Li, H.B., Yu, S., Li, G.L., Deng, H., Xu, B., Ding, J., Gao, J.B., Hong, Y.W., Wong, M.H., 2013. Spatial distribution and historical records of mercury sedimentation in urban lakes under urbanization impacts. Sci. Total Environ. 445–446, 117–125. https://doi.org/10.1016/j.scitotenv.2012.12.041.

Li, H.B., Yu, S., Li, G.L., Liu, Y., Yu, G.B., Deng, H., Wu, S.C., Wong, M.H., 2012b. Urbanization increased metal levels in lake surface sediment and catchment topsoil of waterscape parks. Sci. Total Environ. 432, 202–209. https://doi.org/10.1016/j.scitotenv.2012.05.100.

Liang, P., Wu, S.C., Zhang, J., Cao, Y., Yu, S., Wong, M.H., 2016. The effects of mariculture on heavy metal distribution in sediments and cultured fish around the Pearl River Delta region, south China. Chemosphere 148, 171–177. https://doi.org/10.1016/j.chemosphere.2015.10.110.

Lin, Q., Yu, S., 2018. Losses of natural coastal wetlands by land conversion and ecological degradation in the urbanizing Chinese coast. Sci. Rep. 8, 15046. https://doi.org/10.1038/s41598-018-33406-x.

Liu, S., Shi, X., Yang, G., Khokiattiwong, S., Kornkanitnan, N., 2016. Concentration distribution and assessment of heavy metals in the surface sediments of the western Gulf of Thailand. Environ. Earth Sci. 75, 346. https://doi.org/10.1038/s41598-018-33406-x.

Liu, X., Yu, S., Chen, P.J., Hong, B., Zhang, Y., Lin, X.D., Ma, T., Zhou, T.T., Li, Y.H., 2022. Metal loadings in estuarine bivalve and gastropod shellfish in response to socioeconomic development in watershed. Mar. Environ. Res. 176, 105593. https://doi.org/10.1016/j.marenvres.2022.105593.

Ma, J., Liu, Y., Yu, G., Li, H., Yu, S., Jiang, Y., Li, G., Lin, J., 2016. Temporal dynamics of urbanization-driven environmental changes explored by metal contamination in surface sediments in a restoring urban wetland park. J. Hazard. Mater. 309, 228–235. https://doi.org/10.1016/j.jhazmat.2016.02.017.

Maanan, M., Saddik, M., Maanan, M., Chaibi, M., Assobhei, O., Zourarah, B., 2015. Environmental and ecological risk assessment of heavy metals in sediments of Nador lagoon, Morocco. Ecol. Indic. 48, 616–626. https://doi.org/10.1016/j.ecolind.2014.09.034.

Maul, G.A., Duedall, I.W., 2019. Demography of coastal populations. In: Finkl, C.W., Makowski, C. (Eds.), Encyclopedia of Coastal Science. Encyclopedia of Earth Sciences Series. Springer, Cham https://doi.org/10.1007/978-3-319-93806-6_115.

National Coastal Zone Office of China, 1989. A collection of professional reports on the comprehensive survey of coastal zone and tidal flat resources in China: Environmental Quality Report. China Ocean Press, Beijing.

National Oceanic and Atmospheric Administration of the United States, 1999. Sediment Quality Guidelines Developed for the National Status and Trends Program.

Niu, Y., Jiang, X., Wang, K., Xia, J., Jiao, W., Niu, Y., Yu, H., 2020. Meta analysis of heavy metal pollution and sources in surface sediments of Lake Taihu,China. Sci. Total Environ. 700, 134509. https://doi.org/10.1016/j.scitotenv.2019.134509.

Nour, H.E., El-Sorogy, A.S., Abd El-Wahab, M., Nouh, E.S., Mohamaden, M., Al-Kahtany, K., 2019. Contamination and ecological risk assessment of heavy metals pollution from the Shalateen coastal sediments, Red Sea,Egypt. Mar. Pollut. Bull. 144, 167–172. https://doi.org/10.1016/j.marpolbul.2019.04.056.

Ouyang, W., Wang, Y., Lin, C., He, M., Hao, F., Liu, H., Zhu, W., 2018. Heavy metal loss from agricultural watershed to aquatic system: a scientometrics review. Sci. Total Environ. 637–638, 208–220. https://doi.org/10.1016/j.scitotenv.2018.04.434.

Pan, K., Wang, W.-X., 2012. Trace metal contamination in estuarine and coastal environments in China. Sci. Total Environ. 421, 3–16. https://doi.org/10.1016/j.scitotenv.2011.03.013.

Piva, F., Ciaprini, F., Onorati, F., Benedetti, M., Fattorini, D., Ausili, A., Regoli, F., 2011. Assessing sediment hazard through a weight of evidence approach with bioindicator organisms: a practical model to elaborate data from sediment chemistry, bioavailability, biomarkers and ecotoxicological bioassays. Chemosphere 83, 475–485. https://doi.org/10.1016/j.chemosphere.2010.12.064.

Ren, D.Y., Zhao, F.H., Wang, Y.Q., Yang, S.J., 1999. Distributions of minor and trace elements in Chinese coals. Intl. J. Coal Geol. 40, 109–118. https://doi.org/10.1016/S0166-5162(98)00063-9.

Sany, S.B.T., Salleh, A., Sulaiman, A.H., Sasekumar, A., Rezayi, M., Tehrani, G.M., 2013. Heavy metal contamination in water and sediment of the Port Klang coastal area, Selangor, Malaysia. Environ. Earth Sci. 69, 2013–2025. https://doi.org/10.1007/s12665-012-2038-8.

Sarkodie, S.A., Strezov, V., 2019. A review on environmental Kuznets Curve hypothesis using bibliometric and meta-analysis. Sci. Total Environ. 649, 128–145. https://doi.org/10.1016/j.scitotenv.2018.08.276.

Sharley, D.J., Sharp, S.M., Bourgues, S., Pettigrove, V.J., 2016. Detecting long-term temporal trends in sediment-bound trace metals from urbanised catchments. Environ. Pollut. 219, 705–713. https://doi.org/10.1016/j.envpol.2016.06.072.

Siddique, M.A.M., Rahman, M., Arifur Rahman, S.M., Hassan, M.R., Fardous, Z., Zaman Chowdhury, M.A., Hossain, M.B., 2021. Assessment of heavy metal contamination in the surficial sediments from the lower Meghna River estuary, Noakhali coast, Bangladesh. Int. J. Sediment Res. 36, 384–391. https://doi.org/10.1016/j.ijsrc.2020.10.010.

Simon, E., Baranyai, E., Braun, M., Cserhati, C., Fabian, I., Tothmeresz, B., 2014. Elemental concentrations in deposited dust on leaves along an urbanization gradient. Sci. Total Environ. 490, 514–520. https://doi.org/10.1016/j.scitotenv.2014.05.028.

Song, Q., Li, J., 2014. Environmental effects of heavy metals derived from the e-waste recycling activities in China: a systematic review. Waste Manag. 34, 2587–2594. https://doi.org/10.1016/j.wasman.2014.08.012.

Spencer, K.L., 2002. Spatial variability of metals in the inter-tidal sediments of the Medway Estuary, Kent,UK. Mar. Pollut. Bull. 44, 933–944. https://doi.org/10.1016/S0025-326X(02)00129-7.

Stern, D.I., 2004. The rise and fall of the environmental Kuznets curve. World Dev. 32, 1419–1439. https://doi.org/10.1016/j.worlddev.2004.03.004.

Sun, X., Fan, D., Liu, M., Liao, H., Tian, Y., 2019. Persistent impact of human activities on trace metals in the Yangtze River Estuary and the East China Sea: evidence from sedimentary records of the last 60 years. Sci. Total Environ. 654, 878–889. https://doi.org/10.1016/j.scitotenv.2018.10.439.

Taka, M., Aalto, J., Virkanen, J., Luoto, M., 2016. The direct and indirect effects of watershed land use and soil type on stream water metal concentrations. Water Resour. Res. 52, 7711–7725. https://doi.org/10.1002/2016WR019226.

Tang, Z., Engel, B.A., Pijanowski, B.C., Lim, K.J., 2005. Forecasting land use change and its environmental impact at a watershed scale. J. Environ. Manag. 76, 35–45.

Thapalia, A., Borrok, D.M., van Metre, P.C., Musgrove, M.L., Landa, E.R., 2010. Zn and Cu isotopes as tracers of anthropogenic contamination in a sediment core from an urban lake. Environ. Sci. Technol. 44, 1544–1550. https://doi.org/10.1021/es902933y.

Tran, T.A.M., Leermakers, M., Hoang, T.L., Nguyen, V.H., Elskens, M., 2018. Metals and arsenic in sediment and fish from Cau Hai lagoon in Vietnam: ecological and human health risks. Chemosphere 210, 175–182. https://doi.org/10.1002/2016WR019226.

Trifuoggi, M., Donadio, C., Mangoni, O., Ferrara, L., Bolinesi, F., Nastro, R.A., Stanislao, C., Toscanesi, M., Di Natale, G., Arienzo, M., 2017. Distribution and enrichment of trace metals in surface marine sediments in the Gulf of Pozzuoli and off the coast of the brownfield metallurgical site of Ilva of Bagnoli (Campania, Italy). Mar. Pollut. Bull. 124, 502–511. https://doi.org/10.1016/j.marpolbul.2017.07.033.

USEPA, 2014. EPA, Code of Federal Regulations: Priority Pollutants List. United States Environmental Protection Agency, Washington, DC.

Viers, J., Carretier, S., Auda, Y., Pokrovsky, O.S., Seyler, P., Chabaux, F., Regard, V., Tolorza, V., Herail, G., 2019. Geochemistry of Chilean rivers within the central zone: distinguishing the impact of mining, lithology and physical weathering. Aquat. Geochem. 25, 27–48. https://doi.org/10.1007/s10498-019-09350-1.

von Glasow, R., Jickells, T.D., Baklanov, A., Carmichael, G.R., Church, T.M., Gallardo, L., Hughes, C., Kanakidou, M., Liss, P.S., Mee, L., Raine, R., Ramachandran, P., Ramesh, R., Sundseth, K., Tsunogai, U., Uematsu, M., Zhu, T., 2013. Megacities and large urban agglomerations in the coastal zone: interactions between atmosphere, land, and marine ecosystems. Ambio 42, 13–28. https://doi.org/10.1007/s13280-012-0343-9.

Wang, S., Li, J., Wu, S., Yan, W., Huang, W., Miao, L., Chen, Z., 2016. The distribution characteristics of rare metal elements in surface sediments from four coastal bays on the northwestern South China Sea. Estuar. Coast. Shelf Sci. 169, 106–118. https://doi.org/10.1016/j.ecss.2015.12.001.

Wang, S.L., Xu, X.R., Sun, Y.X., Liu, J.L., Li, H.B., 2013. Heavy metal pollution in coastal areas of South China: a review. Mar. Pollut. Bull. 76, 7–15. https://doi.org/10.1016/j.marpolbul.2013.08.025.

Wang, Y., Zhang, C., Lu, A., Li, L., He, Y., ToJo, J., Zhu, X., 2017. A disaggregated analysis of the environmental Kuznets curve for industrial CO2 emissions in China. Appl. Energy 190, 172–180. https://doi.org/10.1016/j.apenergy.2016.12.109.

Weng, N., Wang, W.X., 2019. Seasonal fluctuations of metal bioaccumulation and reproductive health of local oyster populations in a large contaminated estuary. Environ. Pollut. 250, 175–185. https://doi.org/10.1016/j.envpol.2019.04.019.

Xie, Z., 2020. China's historical evolution of environmental protection along with the forty years' reform and opening-up. Environ. Sci. Ecotechnol.ogy 1, 100001. https://doi.org/10.1016/j.ese.2019.100001.

Yu, S., Wu, Q., Li, Q.L., Gao, J.B., Lin, Q.Y., Ma, J., Xu, Q.F., Wu, S.C., 2014. Anthropogenic land uses elevated metal levels in stream water in a long-term monitored urbanizing watershed. Sci. Total Environ. 488–489, 61–69. https://doi.org/10.1016/j.scitotenv.2014.04.061.

Yuan, Y.Q., Yu, S., Banuelos, G.S., He, Y.F., 2016. Accumulation of Cr, Cd, Pb, Cu, and Zn by plants in tanning sludge storage sites: opportunities for contamination bioindication and phytoremediation. Environ. Sci. Pollut. Res. 23, 22477–22488. https://doi.org/10.1007/s11356-016-7469-4.

Zhang, H., Walker, T.R., Davis, E., Ma, G., 2019a. Ecological risk assessment of metals in small craft harbour sediments in Nova Scotia,Canada. Mar. Pollut. Bull. 146, 466–475. https://doi.org/10.1016/j.marpolbul.2019.06.068.

Zhang, M., He, P., Qiao, G., Huang, J., Yuan, X., Li, Q., 2019b. Heavy metal contamination assessment of surface sediments of the Subei Shoal, China: spatial distribution, source apportionment and ecological risk. Chemosphere 223, 211–222. https://doi.org/10.1016/j.chemosphere.2019.02.058.

Zhao, Y., Yan, M., 1993. Abundance of chemical elements in shallow marine sediment of China. Sci. China B 23, 1084–1090.

Zhou, T.T., Hu, W.W., Yu, S., 2019. Characterizing interactions of socioeconomic development and environmental impact at a watershed scale. Environ. Sci. Pollut. Res. 26, 5680–5692. https://doi.org/10.1007/s11356-018-3875-0.

Zhuang, W., Gao, X., 2014. Assessment of heavy metal impact on sediment quality of the Xiaoqinghe estuary in the coastal Laizhou Bay, Bohai Sea: inconsistency between two commonly used criteria. Mar. Pollut. Bull. 83, 352–357. https://doi.org/10.1016/j.marpolbul.2014.03.039.